Impact of Michaelis–Menten type harvesting of predators in a predator-prey model with Holling type II functional response and Allee effect on prey

Petar Ćirković[a,*], Jelena V. Manojlović[b]

[a]Mathematical Institute of the Serbian Academy of Sciences and Arts
[b]University of Nis, Faculty of Science and Mathematics, Department of Mathematics

Abstract. We propose a predator-prey system with Holling type II functional response incorporating both the Allee effect in the growth of the prey population and a nonlinear Michaelis-Menten type harvesting in predator. We provide a detailed mathematical analysis of the proposed model, including, positivity and boundedness of solutions, uniform persistence, existence, and local and global asymptotic stability of equilibria. Detailed bifurcation analysis is carried out and it is observed that the proposed system exhibits very complex dynamics and many local and global bifurcations as transcritical, pitchfork, saddle-node, Hopf, homoclinic, and Bogdanov-Takens have been identified. We observe the bi-stability and tri-stability in the system, so the basins of attraction in all possible cases of the existence of multiple attractors are discussed in detail. The system shows different types of bi-stabilities behavior in the case of strong and weak Allee effect and different types of tri-stability in the case of strong Allee effect. Extensive numerical simulations are performed for supporting evidence of our analytical findings.

According to our analysis, the proposed model allows the development of a harvesting policy that can prevent the extinction of predator and prey populations. In the case of weak Allee effect, the maximum threshold for continuous predator harvesting without the extinction risk of both species is obtained. In the case of strong Allee effect, the optimal harvesting threshold has been also determined, but optimal harvesting rate of the predator population can only promote the coexistence of the population whenever the Allee effect is quite low, otherwise, the predator harvesting ceases to have any stabilizing effect.

1. Introduction

Over the past few decades, there has been an increasing focus on the interactions between species in population dynamics, particularly in the context of prey-predator relationships. The study of this field has gained interest from a diverse range of communities, including those in biology, ecology, economics,

and the commercial harvesting industry. The mathematical modeling of ordinary differential equations for complex ecological systems has received significant attention since the pioneering research of Lotka [33] and Volterra [45]. Population ecology aims to develop theories and gain insights into the long-time behavior, structure, and coexistence of species, and how they are affected by various factors such as competition, predation, and resource availability.

As in Freedman and Wolkowicz [18], we consider the following system of autonomous ordinary differential equations of the classical Gause type mathematical model of predator-prey interaction

$$\frac{dx}{dt} = xg(x, K) - yp(x),$$
$$\frac{dy}{dt} = y(cp(x) - d),$$

where $x(t)$ and $y(t)$ are densities of the prey and predator at any time $t > 0$, respectively, d is the death rate of the predator, c is the predator's conversion efficiency, $p(x)$ is the functional response, and $g(x, K)$ is the specific per capita growth rate of the prey in the absence of predators. Logistic population growth $g(x, K) = r(1 - x/K)$ is, by far, the most common kind of population growth and occurs when the species population's per capita growth rate is decreased as its size increases. The population's growth rate slows as it approaches carrying capacity K. This leads to the following assumptions on g:

$$g(K, K) = 0, \quad g(0, K) > 0, \quad g_K(0, K) \geq 0, \quad \lim_{K \to \infty} g(0, K) \text{ is finite},$$
$$g_{xK}(0, K) \geq 0, \quad g_x(0, K) \leq 0, \quad \lim_{K \to \infty} g_x(0, K) = 0$$

for all $K > 0$ and

$$g_K(x, K) > 0, \quad g_{xK}(x, K) > 0, \quad g_x(x, K) < 0, \quad \lim_{K \to \infty} g_x(x, K) = 0$$

for all $x > 0, K > 0$ (see [47]). The carrying capacity K bounds above the size of populations which are initially small and tends to pull down populations which are initially large. K is itself a function of the resources such as food, space and sunlight [17].

Functional response is the number of prey successfully attacked per predator as a function of prey density. It describes the way a predator responds to the changing density of its prey. Following C. S. Holling [23, 24], functional responses are generally classified into three types, which are called Holling types I, II, and III (see also [12]). In type I there is a linear relation between prey density and the maximum number of prey killed, while in type II, which is of hyperbolic form, the proportion of prey consumed declines monotonically with prey density. Type III is described by a sigmoid relation expressing the fact that in low densities of prey population, the effect of predation is low, but if the population size increases, the predation is more intensive. In this manuscript, we will use a Holling type II functional response

$$p(x) = \frac{ax}{1 + abx},$$

where x is the prey density, a is predator attack rate, and b represents the handling time (see [10]). It is based on assumption that predators require a certain amount of time to handle each prey, which reduces the time they have available for searching for additional prey. Function $p(x)$ is bounded, monotonically increasing function, and $\lim_{x \to \infty} p(x) = 1/b$, which models the situation where the prey's consumption rate increases as the prey density increases, but in the long run, this growth will be decelerated because of predator's limited capacity in searching and processing food. To enrich model, many researchers modify the nonlinear functional response function, adding some other factors playing important role in the relationships between species in ecosystem like refuge, hunting cooperation, etc. (see [4, 34, 35] and references therein).

The Allee effect is the biological phenomenon of a positive relationship between the population size or density and the per capita growth rate, first observed in 1930. by Allee [3]. In fact, the growth function in the logistic form is a positive function, while the per capita growth rate decreases with density. However, for

many species, low population density may induce many problems. For example, in species where mating or cooperation is necessary for successful reproduction and group defense, individuals may have difficulty finding mates or forming groups when the population size is too small. Additionally, in some cases, individuals may benefit from the presence of conspecifics, for example through increased vigilance against predators, and this benefit may decrease as the population size decreases. It turns out that the growth function of the low-density population is not always positive, and it may be negative when the density of the population is less than the minimum number necessary for the survival of the population, which is called the Allee threshold. The Allee effect may appear due to a wide range of biological phenomena, such as reduced anti-predator vigilance, social thermo-regulation, genetic drift, mating difficulty, reduced defense against the predator, and deficient feeding because of low population densities [42]. There are two types of Allee effect depending on the nature of density dependence at low densities, the strong Allee effect and the weak Allee effect. The distinction between these two types is based on whether or not there exists a threshold population level below which population growth rates become negative. In the case of a strong Allee effect there exists such a threshold population level so that when the population density is below this threshold, the population will be driven to extinction, while above which the population persists. A population with a weak Allee effect has a reduced per capita growth rate at a lower population density or size, but even at this low population size or density, the population will always exhibit a positive per capita growth rate (see [29]).

Mathematically, the Allee effect is usually represented by modifying the growth function. The growth function $F(x) = rx(1 - x/K)(x - m)$ has an enhanced growth rate as the population increases above the Allee effect threshold $m \in (-K, K)$ of the prey species. If $F(0) = 0$ and $F'(0) \geq 0$, as it is the case with $-K \leq m \leq 0$, then $F(x)$ represents prey population exhibits a weak Allee effect, whereas if $F(0) = 0$ and $F'(0) < 0$, as it is the case with $0 < m < K$, then $F(x)$ represents prey population exhibits a strong Allee effect.

The impact of Allee effect in Gauss-type predator-prey model with Holling type II functional response was considered in [21]:

$$
\begin{aligned}
\frac{dN}{dt} &= rN\left(1 - \frac{N}{K}\right)(N - m) - \frac{qNP}{a + N}, \\
\frac{dP}{dt} &= \frac{pNP}{a + N} - dP,
\end{aligned}
\tag{1}
$$

where $N(t)$ and $P(t)$ are densities of the prey and predator populations at any time $t > 0$ respectively. The case of the strong Allee effect and a particular case of the weak Allee effect with $m = 0$ were analyzed. It is observed that strong and weak Allee effects on the prey population perform similar influences on the predator–prey model, thereby increasing the risk of extinction of both species.

From the point of view of human needs, the exploitation of biological resources and the harvesting of populations are commonly practiced in fishery, forestry, and wildlife management [48]. Moreover, harvesting is an important and effective method to prevent and control the oversize growth of predators or prey. A harvesting policy refers to the management of biological resources through the systematic control of the period, intensity, and type of harvesting. The optimal management of renewable resources, which is directly related to sustainable development, has received a lot of attention in recent years from many authors. In the literature, different types of harvesting functions in predator-prey mathematical models have been proposed. The most commonly used are constant, proportional, and nonlinear Michaelis–Menten type harvesting functions (for recent results see [1, 4, 25, 27, 31, 41, 43] and references therein). Harvesting does not always occur with constant yield or constant effort [7]. Also, the proportional harvesting function $h(x) = qEx$ is based on the catch-per-unit-effort hypothesis, where x is the density of the population to be harvested, E is effort applied to harvest individuals which is measured in terms of number of (standard) vessels being used to harvest the individual population, and q is the the catchability coefficient. The proportional harvesting includes several unrealistic features such as the random search for individuals, the equal likelihood of being captured for every individual, unbounded linear increase of h with E for a fixed x, and unbounded linear increase of h with x for a fixed E (see [11]). The nonlinear harvesting term

$$
h(x) = \frac{Eqx}{m_1 E + m_2 x},
$$

proposed first by Clark [9] is called Michaelis-Menten type, where m_1, m_2 are suitable positive constants. These function is more realistic in the sense that the above unrealistic features of proportional harvesting are largely removed as well as from biological and economical points of view (see [22, 28]). In fact, since $h(x) \to qx/m_1$ as $E \to \infty$ and $h(x) \to Eq/m_2$ as $x \to \infty$, the nonlinear harvesting function exhibits saturation effects with respect to both the stock abundance and the effort-level. Also the parameter m_1 is proportional to the ratio of the stock-level to the harvesting rate (catch-rate) at higher levels of effort and m_2 is proportional to the ratio of the effort-level to the harvesting rate (catch-rate) at higher stock-levels. For more details about this kind of harvesting type one can see [11]. Notice also, that if $m_1 = 0$ the nonlinear harvesting term reduces to the case of constant-yield harvesting.

To the best of our knowledge, the simultaneous influence of Allee effect on prey and predator harvesting on Gause-type predator-prey system dynamics with Holling type-II functional response has not been considered in the literature. Thus, the main objective of this paper is to study the impact of the nonlinear Michaelis–Menten type predator harvesting on the dynamics of the system (1). From the ecologic point of view, we will see that the harvesting of predators can be used to control the predator population to prevent the extinction of species. The paper is organized as follows: in Section 2 the model with the nonlinear harvesting is proposed and the system was first reduced to a system with six parameters using proper parameter scaling. The positivity and uniform boundedness are proved, and extinction scenarios have been discussed. The existence and stability of equilibria as well as the uniform persistence of the model in the case of weak Allee effect are discussed in Section 3. The global stability of the origin and predator-free equilibrium points, under some parametric restrictions, has been shown in Section 4. In Section 5 we give the conditions for transcritical, pitchfork, Hopf, and Bogdanov-Takens bifurcations. In Section 6 the numerical simulations have been performed by using MATLAB numerical packages MatCont [13] and Phase Plane and Slope Field apps [49] in order to validate the theoretical findings and to visualize the dynamical behavior of the system. In Section 7 we provide a detailed discussion of basins of attraction of multiple attractors. We conclude the paper in sections 8 and 9 by giving a summary of the obtained results and their ecological implications, as well as a comparison of the dynamics of the proposed model with the strong and weak Allee effect.

2. Mathematical model

Starting from the conclusions in [21] that the Allee effect can increase the risk of extinction, the combined impact of Allee effect on prey and harvesting in predator on population dynamics of predator-prey interactions may lead to a better understanding of conditions that may lead to predator and prey extinction. Consequently, this paper aims to give a detailed analysis of a mathematical model for a predator–prey system with Holling type II functional response, the Allee effect in the growth of the prey population, and a nonlinear Michaelis–Menten type harvesting in predator:

$$
\begin{aligned}
\frac{dN}{dT} &= rN\left(1 - \frac{N}{K}\right)(N - m) - \frac{aNP}{1 + abN}, \\
\frac{dP}{dT} &= \frac{\theta aNP}{1 + abN} - dP - \frac{EqP}{m_1 E + m_2 P},
\end{aligned}
\tag{2}
$$

where $N(T)$ and $P(T)$ are densities of the prey and predator populations at any time $T > 0$ respectively, r is the intrinsic growth rate of the prey, K is the prey carrying capacity, m is the Allee effect threshold of the prey species, a is predator attack rate, b is the handling time, θ is predator's conversion efficiency, $\theta \in (0, 1)$, d is the death rate of the predator, E is effort applied to harvest individuals, q is the catch rate, m_1, m_2 are suitable positive constants.

In order to reduce the number of parameters for stability and bifurcation analysis we use the transformation

$$
x = \frac{N}{K}, \quad y = \frac{P}{rbK^2}, \quad t = rKT,
$$

so that we can write the model (2) in terms of dimensionless variables and parameters as follows,

$$
\begin{aligned}
\frac{dx}{dt} &= x(1-x)(x-\mu) - \frac{xy}{\alpha+x} = xg_1(x,y),\\
\frac{dy}{dt} &= \frac{\beta xy}{\alpha+x} - \delta y - \frac{hy}{e+y} = yg_2(x,y),
\end{aligned}
\tag{3}
$$

where

$$
\mu = \frac{m}{K}, \quad \alpha = \frac{1}{abK}, \quad \beta = \frac{\theta}{br}, \quad \delta = \frac{d}{rK}, \quad h = \frac{Eq}{m_2br^2K^3}, \quad e = \frac{m_1E}{m_2rbK^2},
$$

and

$$
g_1(x,y) = (1-x)(x-\mu) - \frac{y}{\alpha+x}, \quad g_2(x,y) = \frac{\beta x}{\alpha+x} - \delta - \frac{h}{e+y}.
$$

We note that $-1 \le \mu \le 1$, so $-1 \le \mu \le 0$ indicates the presence of a weak Allee effect affecting the prey, while $0 < \mu \le 1$ indicates the presence of a strong Allee effect.

2.1. Positivity and boundedness of solutions

First, we prove the positivity and the boundedness of the solutions of the system (3) starting from an interior point of the first quadrant.

Theorem 2.1. *All solutions of the system* (3) *with positive initial values remain positive for all $t \ge 0$.*

Proof. Integrating both equations of the system (3), we get

$$
x(t) = x(0)\exp\left(\int_0^t g_1(x(s),y(s))ds\right), \quad y(t) = y(0)\exp\left(\int_0^t g_2(x(s),y(s))ds\right), \quad t \ge 0
$$

so that $x(t)$ and $y(t)$ are always nonnegative provided that $x(0) > 0$ and $y(0) > 0$. Therefore, all the solutions of the system starting from an interior point of the first quadrant will remain in the first quadrant for all future time. $\square$

Theorem 2.2. *All solutions of the system* (3) *with positive initial values are uniformly bounded for sufficiently large $t \ge 0$.*

Proof. We consider $(x(t), y(t))$ be any positive solution of the system (3) satisfying initial conditions $x(0) > 0$ and $y(0) > 0$. First, we prove that the boundedness of the solution $x(t)$. The following two cases are possible: $x(0) \le 1$ and $x(0) > 1$.

(i) Suppose that $x(0) \le 1$. We will prove that $x(t) \le 1$ for all $t \ge 0$. Let us assume that is not true i.e. there exist $t_1, t_2 > 0$ such that $x(t_1) = 1$ and $x(t) > 1$ for all $t \in (t_1, t_2)$. Then, $g_1(x(s), y(s)) < 0$ for all $s \in (t_1, t_2)$, so that for all $t \in (t_1, t_2)$

$$
\begin{aligned}
x(t) &= x(0)\exp\left(\int_0^t g_1(x(s),y(s))ds\right) = x(0)\exp\left(\int_0^{t_1} g_1(x(s),y(s))ds\right)\exp\left(\int_{t_1}^t g_1(x(s),y(s))ds\right)\\
&= x(t_1)\exp\left(\int_{t_1}^t g_1(x(s),y(s))ds\right) < 1,
\end{aligned}
$$

which is a contradiction to our assumption. Hence, $x(t) \le 1$ for all $t \ge 0$.

(ii) Suppose that $x(0) > 1$. If there exists $t_0 > 0$ such that $x(t_0) \le 1$ then, as in the first case, we conclude that $x(t) \le 1$ for all $t > t_0$. If $x(t) > 1$ for all $t \ge 0$, then $g_1(x(s), y(s)) < 0$ for $s \ge 0$ and

$$
x(t) = x(0)\exp\left(\int_0^t g_1(x(s),y(s))ds\right) \le x(0).
$$

Therefore, from cases (i) and (ii), we conclude that $x(t) \leq \max\{x(0), 1\}$, $t \geq 0$, so that $x_M \stackrel{\text{def}}{=} \limsup_{t\to\infty} x(t) < \infty$. Now, from the first equation in (3), we have

$$\frac{dx}{dt} \leq (x_M - \mu)x(1 - x),$$

implying that $\limsup_{t\to\infty} x(t) \leq 1$.

To show that the system is uniformly bounded, let $Q(x(t), y(t)) = \beta x(t) + y(t)$. Then

$$\frac{dQ}{dt} = \beta x'(t) + y'(t) \leq \beta x(1 - x)(x - \mu) - \delta y \leq \beta x \left(\frac{1 - \mu}{2}\right)^2 - \delta y$$

where $\left(\frac{1-\mu}{2}\right)^2$ is the maximum of the quadratic function $(1 - x)(x - \mu)$. Using $x_M \leq 1$, we obtain

$$\frac{dQ}{dt} \leq \beta x \left(\left(\frac{1 - \mu}{2}\right)^2 + \delta\right) - \delta Q \leq W - \delta Q,$$

where $W \stackrel{\text{def}}{=} \beta \left(\left(\frac{1-\mu}{2}\right)^2 + \delta\right)$ is positive constant. Then,

$$0 < Q(x(t), y(t)) \leq \frac{W}{\delta} + \left(Q(x(0), y(0)) - \frac{W}{\delta}\right) e^{-\delta t}, \quad t \geq 0$$

which implies that $\limsup_{t\to\infty} Q(t) \leq \frac{W}{\delta}$. Therefore, all solutions of the system (3) enter into the region

$$\Omega = \left\{(x, y) \in \mathbb{R}_+^2 : 0 \leq x(t) \leq 1, \ 0 \leq \beta x(t) + y(t) \leq \frac{W}{\delta} + \varepsilon, \varepsilon > 0\right\},$$

which means that all solutions starting in $\mathbb{R}_+^2$ remain uniformly bounded for all time. $\square$

2.2. Extinction of species

Next, we give the extinction criteria of prey and predator species. Let

$$x_M = \limsup_{t\to\infty} x(t), \quad y_m = \liminf_{t\to\infty} y(t), \quad y_M = \limsup_{t\to\infty} y(t).$$

Theorem 2.3. *If $\mu > 0$ and $x_M < \mu$, then $\lim_{t\to\infty} x(t) = 0$.*

Proof. Let $\varepsilon > 0$ such that $\varepsilon < \mu - x_M$. It follows that there exist $t_0 > 0$ such that $x(t) < x_M + \varepsilon$ for $t > t_0$. For $t > t_0$, the first equation in (3) implies

$$\frac{dx}{dt} < x(1 - x)(x - \mu) < x(x_M + \varepsilon - \mu).$$

Since $x_M + \varepsilon - \mu < 0$, it follows that $\lim_{t\to\infty} x(t) = 0$. $\square$

Theorem 2.4. *If $y_m > 2(1 + \alpha)$, then $\lim_{t\to\infty} x(t) = 0$.*

Proof. Let $\varepsilon > 0$ such that $\varepsilon < 1 - \mu$. It follows that there exist $t_1 > 0$ such that $x(t) < 1 + \varepsilon$ for $t > t_1$. Also for $0 < \varepsilon_1 < y_m - 2(1 + \alpha)$, there exist $t_2 \geq t_1$, such that $y(t) > y_m - \varepsilon_1$ for $t > t_2$. For $t > t_2$, the first equation in (3) implies

$$\frac{dx}{dt} < x\left((\mu + 1)x - \mu - \frac{y}{\alpha + x}\right) < x\left((\mu + 1)(1 + \varepsilon) - \mu - \frac{y_m - \varepsilon_1}{\alpha + 1}\right) < x\left(2 - \mu^2 - \frac{y_m - \varepsilon_1}{\alpha + 1}\right) < x\left(2 - \frac{y_m - \varepsilon_1}{\alpha + 1}\right).$$

Since $\varepsilon_1 < y_m - 2(1 + \alpha)$, it follows that $\lim_{t\to\infty} x(t) = 0$. $\square$

Theorem 2.5. *If* $\lim_{t\to\infty} x(t) = 0$, *then* $\lim_{t\to\infty} y(t) = 0$.

Proof. Suppose $\lim_{t\to\infty} x(t) = 0$. For $\varepsilon = \frac{\alpha\delta}{2\beta}$ there exists $t_0 \geq 0$ such that $x(t) < \varepsilon$ for all $t \geq t_0$. The second equation of (3) implies

$$\frac{dy}{dt} < y\left(\frac{\beta\varepsilon}{\alpha} - \delta\right) = -\frac{\delta}{2}y, \quad t \geq t_0.$$

Hence $\lim_{t\to\infty} y(t) = 0$. $\quad\square$

Theorem 2.6. *Let* $h > e\left(1 + \frac{\beta}{\alpha}\right)$. *If* $y_M < \frac{h\alpha}{\beta+\alpha} - e$, *then* $\lim_{t\to\infty} y(t) = 0$.

Proof. Choose $\varepsilon > 0$ such that $\varepsilon < \frac{\alpha}{\beta}$. It follows that there exist $t_1 > 0$ such that $x(t) < 1 + \varepsilon$ for $t > t_1$. Also for $0 < \varepsilon_1 < \frac{h\alpha}{\beta+\alpha} - e - y_M$, there exist $t_2 \geq t_1$, such that $y(t) < y_M + \varepsilon_1$ for $t > t_2$. For $t > t_2$, the second equation in (3) implies

$$\frac{dy}{dt} < y\left(\frac{\beta(1+\varepsilon)}{\alpha} - \frac{h}{e+y}\right) < y\left(\frac{\beta}{\alpha} + 1 - \frac{h}{e+y_M+\varepsilon_1}\right) < \frac{y}{\alpha(e+y_M+\varepsilon_1)}[(\beta+\alpha)(e+y_M+\varepsilon_1) - h\alpha].$$

Since $\varepsilon_1 < \frac{h\alpha}{\beta+\alpha} - e - y_M$, it follows that $\lim_{t\to\infty} y(t) = 0$. $\quad\square$

It is concluded from previous results that in the case of strong Allee effect, if the density of the prey population is below the Allee effect threshold μ, then the prey population will go extinct (by Theorem 2.3). Also, since the condition in Theorem 2.4 is equivalent to $\liminf_{t\to\infty} aP(t) > 2r(1 + abK)$, we conclude that if the predator consumes prey with a higher rate, the prey population will go extinct. According to Theorem 2.5 the extinction of the prey population leads to the extinction of the predator population. By Theorem 2.6 it is concluded that if the harvesting rate of predators is above the threshold $e(1 + \beta/\alpha)$, then if the density of the predator population is below the threshold $\frac{h\alpha}{\beta+\alpha} - e$, the predator population will extinct with time.

3. Existence and stability of equilibria

3.1. Existence of equilibria

The axial equilibrium points of the system (3) in the case of strong Allee effect are trivial equilibrium $E_0(0,0)$ and two predator-free equilibria $E_1(1,0)$, $E_\mu(\mu,0)$, while in the case of weak Allee effect trivial equilibrium $E_0(0,0)$ and predator free equilibrium $E_1(1,0)$ are the only axial equilibria. To obtain the
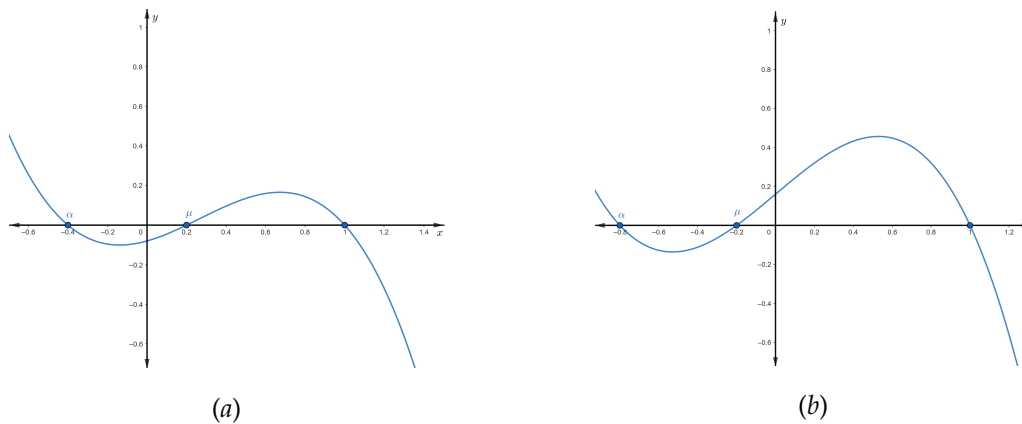

Figure 1: **(a)** $0 < \mu < 1$ **(b)** $\mu < 0$

possible number of interior equilibrium points, we consider the non-trivial prey nullcline given by

$$y = (1 - x)(x - \mu)(x + \alpha) = \pi_1(x),$$ (4)

whose graphics is shown in Figure 1, and the non-trivial predator nullcline given by

$$y = \frac{h(x + \alpha)}{\beta x - \delta(x + \alpha)} - e = \pi_2(x).$$ (5)

It is clear that prey nullcline has a local maximum at

$$x_{max} = \frac{1}{3}\left(1 - \alpha + \mu + \sqrt{1 + \alpha + \alpha^2 - \mu + \mu\alpha + \mu^2}\right)$$ (6)

such that $\mu < x_{max} < 1$. From (5) we have

$$\frac{dy}{dx} = -\frac{h\alpha\beta}{((\beta - \delta)x - \alpha\delta)^2}$$

which implies that the non-trivial predator nullcline is decreasing function. When $\beta \neq \delta$ the vertical asymptote of prey nullcline is $x = \frac{\alpha\delta}{\beta - \delta}$, the horizontal asymptote is $y = \frac{h - e(\beta - \delta)}{\beta - \delta}$ and it intersects x-axis at the point $B(x_B, 0)$, $x_B = \frac{\alpha(h + e\delta)}{e(\beta - \delta) - h}$. The number of interior equilibria depends on the position of these asymptotes and the point B.

$(a)\,\beta > \delta, h \geq e(\beta - \delta)$

$(b)\,\beta > \delta, h < e(\beta - \delta)$

$(c)\,\beta = \delta$

$(d)\,\beta < \delta$
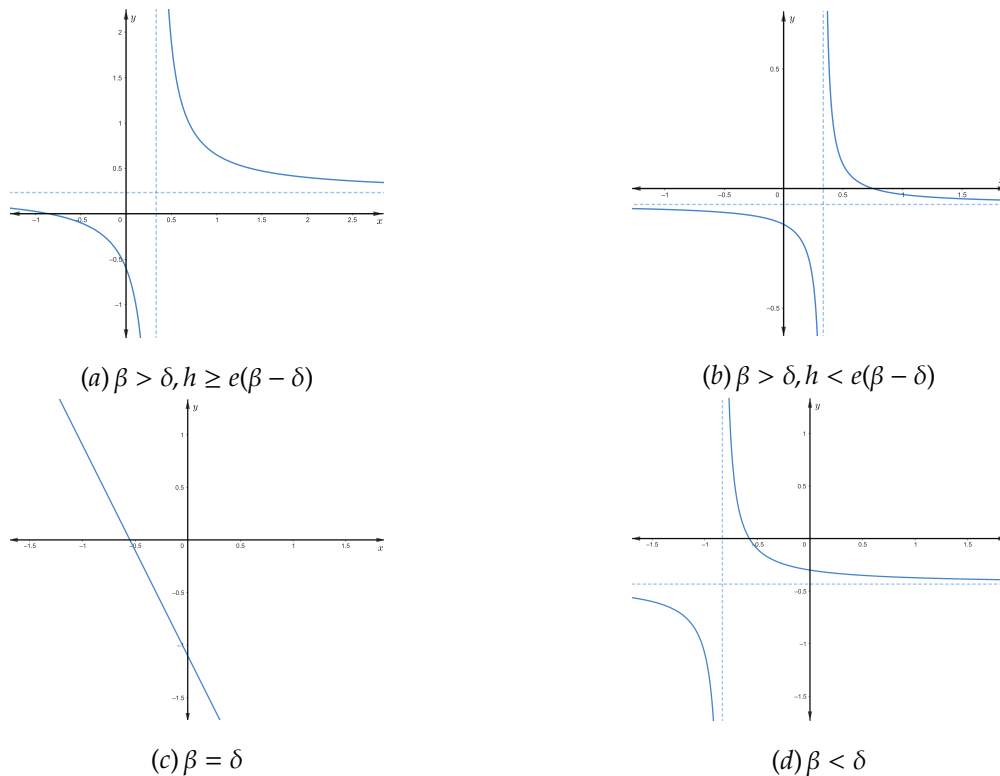
Figure 2: The non-trivial predator nullcline.

(i) If $\beta > \delta, h \geq e(\beta - \delta)$, the vertical asymptote is on the right side of the y-axis, the horizontal asymptote is above the x-axis or lying on it and there is no intersection of prey nullcline with positive part of
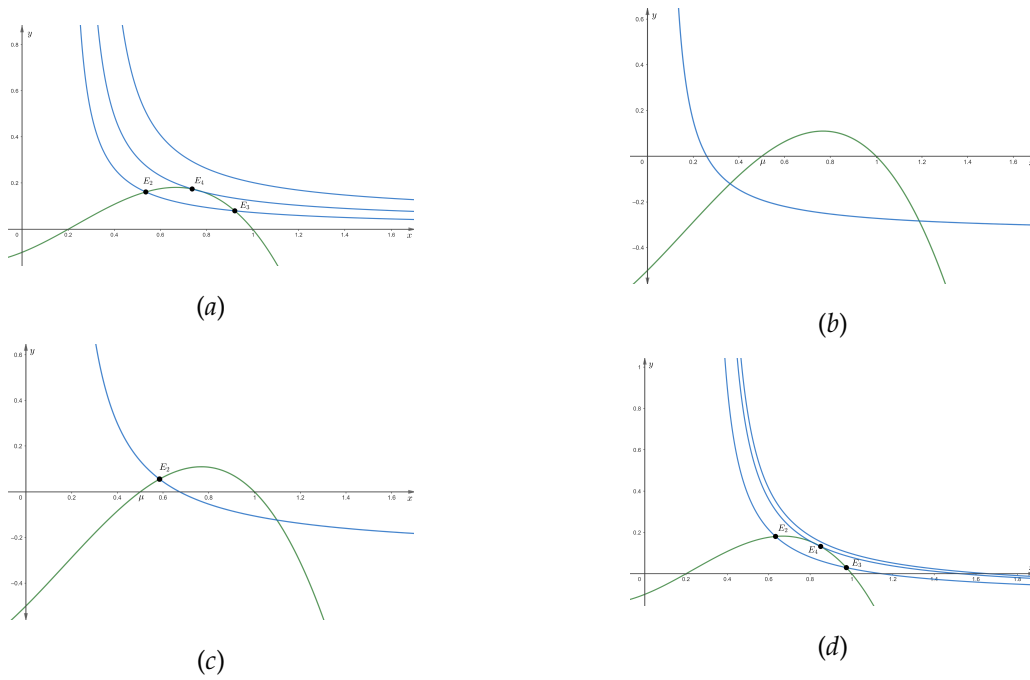
(a)

(b)

(c)

(d)

Figure 3: The possible number of interior equilibria depending on the behavior of predator (blue) and prey (green) non-trivial nullclines in the case of the strong Allee effect.

x-axis (Fig. 2-(a)). Thus, the non-trivial predator and prey nullclines can have two intersection points in the first quadrant, or they touch each other at the unique interior equilibrium, or they don't have intersection points in the first quadrant (Fig. 3-(a)).

(ii) If $\beta > \delta, h < e(\beta - \delta)$, the vertical asymptote is on the right side of the y-axis, the horizontal asymptote is below the x-axis and the non-trivial predator nullcline intersects positive part of x-axis at the point B (Fig. 2-(b)). In this case, the number of interior equilibria depends on the relative position of the point B to the points E_1 and E_μ.

In the case of strong Allee effect, we distinguish three cases:

(ii-1) If B is to the left of the point E_μ or these two points coincide i.e. if

$$x_B \le \mu \quad \Rightarrow \quad h \le e\left(\frac{\beta\mu}{\alpha + \mu} - \delta\right) = H_1,$$

then the non-trivial nullclines do not intersect in the first quadrant (Fig. 3-(b)).

(ii-2) If B is between points E_μ and E_1 or points B and E_1 coincide, that is

$$\mu < x_B \le 1 \quad \Rightarrow \quad H_1 = e\left(\frac{\beta\mu}{\alpha + \mu} - \delta\right) < h \le e\left(\frac{\beta}{\alpha + 1} - \delta\right) = H_2, \tag{7}$$

then the non-trivial predator and prey nullclines intersect at the unique interior equilibrium (Fig. 3-(c)).

(ii-3) If B is to the right of the point E_1 i.e. if

$$x_B > 1 \quad \Rightarrow \quad h > e\left(\frac{\beta}{\alpha + 1} - \delta\right) = H_2, \tag{8}$$

then the non-trivial nullclines can have two intersection points in the first quadrant, or they touch each other at the unique interior equilibrium, or they don't have intersection points in the first quadrant (Fig. 3-(d)).

In the case of weak Allee effect, only the following two cases are possible:

(ii-a) If B is to the left of the point E_1 or points B and E_1 coincide, that is as in (7), if $h \le H_2$, then the non-trivial predator and prey nullclines intersect at the unique interior equilibrium.

(ii-b) If B is to the right of the point E_1, that is as in (8) if $h > H_2$, then the non-trivial nullclines can have two intersection points in the first quadrant, or they touch each other at the unique interior equilibrium, or they don't have intersection points in the first quadrant.

We note that $H_2 = e\left(\frac{\beta}{\alpha+1} - \delta\right) < e(\beta - \delta)$ and if $\mu > 0$, then $H_1 < H_2$.

(iii) When $\beta = \delta$ the prey nullcline is the line $y = -\frac{h}{\alpha\delta}x - \frac{1}{\delta}$ whose points do not belong to the first quadrant (Fig. 2-(c)). Hence, the non-trivial predator and prey nullclines do not intersect in the first quadrant.

(iv) When $\beta < \delta$, it follows that $h > e(\beta - \delta)$. The vertical asymptote is on the left side of the y-axis and the horizontal asymptote is below the x-axis. In this case, the prey nullcline does not pass through the first quadrant (Fig. 2-(d)) and the non-trivial predator and prey nullclines do not intersect in the first quadrant.

By summarizing the above results, we can formulate the following theorem.

Theorem 3.1. *In the case of strong Allee effect the system* (3) *doesn't have an interior equilibrium for $\beta \le \delta$. If $\beta > \delta$, then:*

(i) *there is no interior equilibrium, if $0 < h \le H_1$;*

(ii) *there is a unique interior equilibrium E_2, if $H_2 > 0$ and $H_1 < h \le H_2$;*

(iii) *there is either no interior equilibrium or an unique interior equilibrium E_4 or two interior equilibria E_2 and E_3, if $h > H_2$.*

Theorem 3.2. *In the case of weak Allee effect the system* (3) *doesn't have an interior equilibrium for $\beta \le \delta$. If $\beta > \delta$ then:*

(i) *there is an unique interior equilibrium E_2, if $0 < h \le H_2$;*

(ii) *there is either no interior equilibrium or an unique interior equilibrium E_4 or two interior equilibria E_2 and E_3, if $h > H_2$.*

3.2. Stability Analysis

First, we discuss the local asymptotic stability properties of the axial equilibrium points. The Jacobian matrix of the system (3) evaluated at arbitrary point (x, y) is

$$J(x, y) = \begin{pmatrix} -3x^2 + \left(2 + \frac{y}{(x+\alpha)^2} + 2\mu\right)x - \frac{y}{x+\alpha} - \mu & -\frac{x}{x+\alpha} \\ \frac{\alpha\beta y}{(x+\alpha)^2} & \frac{\beta x}{x+\alpha} - \delta - \frac{eh}{(e+y)^2} \end{pmatrix}. \tag{9}$$

Theorem 3.3. *Trivial equilibrium E_0 is*

(i) *a stable node if $0 < \mu < 1$,*

(ii) *a saddle if $\mu < 0$.*

Proof. The Jacobian matrix

$$J(E_0) = \begin{pmatrix} -\mu & 0 \\ 0 & -\frac{h+e\delta}{e} \end{pmatrix}$$

has eigenvalues $\lambda_1 = -\frac{h+e\delta}{e} < 0$ and $\lambda_2 = -\mu$. For $\mu > 0$ both eigenvalues are negative, so that E_0 is a stable node, for $\mu < 0$ eigenvalues have opposite sign, so that E_0 is a saddle. $\square$

Theorem 3.4. *The predator free equilibrium $E_1(1,0)$ is*

(i) *a stable node if $h > H_2 = e\left(\frac{\beta}{\alpha+1} - \delta\right)$;*

(ii) *a saddle if $0 < h < H_2 = e\left(\frac{\beta}{\alpha+1} - \delta\right)$;*

(iii) *a saddle-node if $h = H_2 > 0$ and $\beta \neq \widehat{\beta_2}$; Further, if either $(\alpha+1)^2(1-\mu) - \alpha e < 0$ or $(\alpha+1)^2(1-\mu) - \alpha e > 0$ and $\beta < \widehat{\beta_2}$, a stable parabolic sector is on the right side of E_1. If $(\alpha+1)^2(1-\mu) - \alpha e > 0$ and $\beta > \widehat{\beta_2}$, a stable parabolic sector is on the left side of E_1.*

(iv) *a stable node for $\beta = \widehat{\beta_2} > 0$ and $h = H_2 > 0$,*

where

$$\widehat{\beta_2} = \frac{\delta(\alpha+1)^3(1-\mu)}{(\alpha+1)^2(1-\mu) - \alpha e}. \tag{10}$$

Proof. The Jacobian matrix

$$J_1 = J(E_1) = \begin{pmatrix} \mu - 1 & -\frac{1}{1+\alpha} \\ 0 & \frac{\beta}{1+\alpha} - \frac{h}{e} - \delta \end{pmatrix}$$

has eigenvalues

$$\lambda_1 = \frac{\beta}{\alpha+1} - \delta - \frac{h}{e}, \quad \lambda_2 = \mu - 1 < 0.$$

If $h > H_2$, then $\lambda_1 < 0$, so E_1 is a stable node and if $h < H_2$, then $\lambda_1 > 0$, so E_1 is a saddle.

Next, consider the case when $h = H_2 > 0$, so that $\det(J_1) = 0$ and $\operatorname{tr}(J_1) = \mu - 1 < 0$. By translating E_1 to the origin and expanding obtained system in Taylor series, we get a system

$$\begin{aligned} \frac{dx}{dt} &= (\mu-1)x - \frac{y}{\alpha+1} + (\mu-2)x^2 - \frac{\alpha}{(\alpha+1)^2}xy - x^3 + \frac{\alpha}{(\alpha+1)^3}x^2y + O(\|x,y\|^3), \\ \frac{dy}{dt} &= \frac{\alpha\beta}{(\alpha+1)^2}xy + \frac{\beta - \alpha\delta - \delta}{(\alpha+1)e}y^2 - \frac{\alpha\beta}{(\alpha+1)^3}x^2y + \frac{\alpha\delta - \beta + \delta}{(\alpha+1)e^2}y^3 + O(\|x,y\|^3). \end{aligned} \tag{11}$$

Afterwards, by applying the coordinate transformation and time reparametrization

$$X = \frac{x}{(\alpha+1)(\mu-1)} + y, \quad Y = x, \quad \tau = (\mu-1)t,$$

the system (11) becomes

$$\begin{aligned} \frac{dX}{d\tau} &= P_1(X,Y) = a_{20}X^2 + a_{11}XY + a_{30}X^3 + a_{21}X^2Y + a_{12}XY^2 + a_{03}Y^3 + O(\|X,Y\|^4), \\ \frac{dY}{d\tau} &= P_2(X,Y) = Y + b_{20}X^2 + b_{11}XY + b_{02}Y^2 + b_{30}X^3 + b_{21}X^2Y + b_{12}XY^2 + b_{03}Y^3 + O(\|X,Y\|^4), \end{aligned} \tag{12}$$

where

$$a_{20} = \frac{(\alpha+1)^2(1-\mu)(\delta(\alpha+1) - \beta) + \alpha\beta e}{(\alpha+1)^3 e(\mu-1)^2}, \quad a_{11} = \frac{\alpha\beta}{(\alpha+1)^2(\mu-1)},$$

$$a_{30} = \frac{(\alpha+1)^4(\mu-1)^2(\alpha\delta - \beta + \delta) - e^2\alpha\beta}{e^2(1+\alpha)^5(\mu-1)^3}, \quad a_{21} = -\frac{2\alpha\beta}{(\alpha+1)^4(\mu-1)^2}, \quad a_{12} = \frac{\alpha\beta}{(\alpha+1)^3(1-\mu)},$$

$$b_{20} = \frac{(\alpha + 1)^2(\mu - 1)(\delta(\alpha + 1) - \beta) + e(-\alpha(\alpha + \beta + 3) + (\alpha + 1)\mu - 2)}{(\alpha + 1)^4 e(\mu - 1)^3},$$

$$b_{11} = \frac{-\alpha(3\alpha + \beta + 7) + \alpha(\alpha + 3)\mu + 2(\mu - 2)}{(\alpha + 1)^3(\mu - 1)^2}, \quad b_{02} = \frac{\mu - 2}{\mu - 1}, \quad b_{03} = \frac{1}{1 - \mu}$$

$$b_{30} = \frac{e^2(\alpha\beta + \alpha(\alpha + 1)(\mu - 1) - (1 + \alpha)^3) - (\alpha + 1)^4(\mu - 1)^2(\alpha\delta - \beta + \delta)}{e^2(1 + \alpha)^6(\mu - 1)^4}$$

$$b_{21} = \frac{\alpha(\alpha(-3\alpha + 2\mu - 11) + 2\beta + 2\mu - 11) - 3}{(\alpha + 1)^5(\mu - 1)^3}, \quad b_{12} = \frac{\alpha(\alpha(-3\alpha + \mu - 10) + \beta + \mu - 10) - 3}{(\alpha + 1)^4(\mu - 1)^2}.$$

The coefficient a_{20} of X^2 in the first equation in (12) is not equal to zero if $\beta \neq \widehat{\beta_2}$, so it follows, by Theorem 7.1 in [50], that E_1 is a saddle-node. Sign of $\widehat{\beta_2}$ depends on $M = (\alpha + 1)^2(1 - \mu) - \alpha e$. If either $M < 0$ or $M > 0$ and $\beta < \widehat{\beta_2}$, we have that $a_{20} > 0$ and a stable parabolic sector is on the right side of E_1. If $M > 0$ and $\beta > \widehat{\beta_2}$, we have that $a_{20} < 0$ and a stable parabolic sector is on the left side of E_1.

Finally, consider the case $h = H_1 > 0$ and $\beta = \widehat{\beta_2} > 0$. Suppose that the center manifold of the system (12) has a form $Y = H(X) = c_2 X^2 + c_3 X^3 + o(|X|^4)$. From

$$P_1(X, H(X)) \frac{dH(X)}{dX} - P_2(X, H(x)) = 0$$

we obtain coefficients

$$c_2 = -b_{20}\Big|_{\beta = \widehat{\beta_2}}, \quad c_3 = b_{11}b_{20} - b_{30}\Big|_{\beta = \widehat{\beta_2}}.$$

Therefore, the restriction of the system (12) to the center manifold has the following form

$$\frac{dX}{d\tau} = P_1(X, H(x)) = (a_{30} - a_{11}b_{20})X^3 = \frac{\alpha\delta\left(e(\alpha + 1 + 2(1 - \mu)) + (\alpha + 1)^2(1 - \mu)^2\right)}{e(\alpha + 1)^2(1 - \mu)^3\left((1 - \mu)(\alpha + 1)^2 - e\alpha\right)}X^3 + O(|X|^4).$$

The condition $\widehat{\beta_2} > 0$ implies that $(\alpha + 1)^2(1 - \mu) - \alpha e > 0$, so that the coefficient with X^3 in this restriction is positive. We used a time transformation $\tau = (\mu - 1)t$, so using Theorem 7.1 in [50], we conclude that E_1 is a stable node. $\square$

Theorem 3.5. *If $\mu \in (0, 1)$, the predator free equilibrium $E_\mu(\mu, 0)$ is*

(i) *an unstable node for $0 < h < H_1 = e\left(\frac{\beta\mu}{\alpha+\mu} - \delta\right)$;*

(ii) *a saddle for $h > H_1 = e\left(\frac{\beta\mu}{\alpha+\mu} - \delta\right)$;*

(iii) *a saddle-node for $h = H_1 > 0$, with an unstable parabolic sector on the right side of E_μ, so that E_μ is a repelling saddle-node.*

Proof. The Jacobian matrix

$$J_\mu = J(E_\mu) = \begin{pmatrix} \mu(1 - \mu) & -\frac{\mu}{\mu+\alpha} \\ 0 & \frac{\beta\mu}{\mu+\alpha} - \frac{h}{e} - \delta \end{pmatrix}$$

has eigenvalues

$$\lambda_1 = \frac{\beta\mu}{\mu + \alpha} - \frac{h}{e} - \delta, \quad \lambda_2 = \mu(1 - \mu) > 0$$

If $h < H_1$, then $\lambda_1 > 0$, so that E_μ is an unstable node, and if $h > H_1$, then $\lambda_1 < 0$, so that E_μ is a saddle. Next, consider the case when $h = H_1 > 0$. In this case $\det(J_\mu) = 0$ and $\mathrm{tr}(J_\mu) = \mu(1 - \mu) > 0$. By translating E_μ to the origin and expanding obtained system in Taylor series, we obtain the system

$$
\begin{aligned}
\frac{dx}{dt} &= \mu(1 - \mu)x - \frac{\mu}{\alpha + \mu}y + (1 - 2\mu)x^2 - \frac{\alpha}{(\alpha + \mu)^2}xy + O(\|x, y\|^3) \\
\frac{dy}{dt} &= \frac{\alpha\beta}{(\alpha + \mu)^2}xy + \frac{\beta\mu - \alpha\delta - \delta\mu}{e(\alpha + \mu)}y^2 + O(\|x, y\|^3).
\end{aligned}
\tag{13}
$$

Afterwards, by applying the coordinate transformation and time reparametrization

$$
X = -\frac{x}{(\alpha + \mu)(\mu - 1)} + y, \quad Y = x, \quad \tau = \mu(1 - \mu)t,
$$

the system (13) becomes

$$
\begin{aligned}
\frac{dX}{d\tau} &= a_{20}X^2 + a_{11}XY + O(\|X, Y\|^3), \\
\frac{dY}{d\tau} &= Y + b_{20}X^2 + b_{11}XY + b_{02}Y^2 + O(\|X, Y\|^3),
\end{aligned}
$$

where

$$
a_{20} = \frac{(\mu - 1)(\alpha + \mu)^2(\delta(\alpha + \mu) - \beta\mu) + \alpha\beta e}{e(\mu - 1)^2\mu(\alpha + \mu)^3}, \quad a_{11} = \frac{\alpha\beta}{(1 - \mu)\mu(\alpha + \mu)^2},
$$

$$
b_{20} = \frac{(\mu - 1)(\alpha + \mu)^2(\delta(\alpha + \mu) - \beta\mu) + e\alpha\beta + e\mu(\alpha + \mu)(2\mu + \alpha - 1)}{e(\mu - 1)^3\mu(\alpha + \mu)^4},
$$

$$
b_{11} = \frac{\alpha(\alpha - \beta) + (2 - 7\alpha)\mu^2 - 3(\alpha - 1)\alpha\mu - 4\mu^3}{(\mu - 1)^2\mu(\alpha + \mu)^3}, \quad b_{02} = \frac{2\mu - 1}{(\mu - 1)\mu}.
$$

The condition $H_1 > 0$ implies that $\beta\mu - \delta(\alpha + \mu) > 0$, so that the coefficient $a_{20} > 0$. By Theorem 7.1 in [50], we conclude that E_μ is saddle-node with an unstable parabolic sector on the right side of E_μ, so that E_μ is a repelling saddle-node. $\square$

Overview of the existence and stability conditions for the axial equilibrium points of the system (3) is discussed in tables 1 and 2.

Condition	$E_0(0, 0)$	$E_1(1, 0)$	$E_\mu(\mu, 0)$
$\beta \leq \delta$	stable node	stable node	saddle
$\beta > \delta, 0 < h < H_1$	stable node	saddle	unstable node
$\beta > \delta, 0 < h = H_1$	stable node	saddle	saddle-node
$\beta > \delta, H_2 > 0, H_1 < h < H_2$	stable node	saddle	saddle
$\beta > \delta, 0 < h = H_2, \beta \neq \widehat{\beta_2}$	stable node	saddle-node	saddle
$\beta > \delta, 0 < h = H_2, \beta = \widehat{\beta_2}$	stable node	stable node	saddle
$\beta > \delta, h > H_2$	stable node	stable node	saddle

Table 1: Summary of the stability of axial equilibria in the case of a strong Allee effect.

Further, we discuss the local asymptotic stability properties of the interior equilibrium points $E_i(x_i, y_i)$, $i = 2, 3, 4$, where $y_i = (1 - x_i)(\alpha + x_i)(x_i - \mu)$. Since $g_1(x_i, y_i) = g_2(x_i, y_i) = 0$, $i = 2, 3, 4$, the Jacobian matrix of the system (3) at arbitrary interior point E_i, is given by

$$
J_i = J(x_i, y_i) = \begin{pmatrix} x_i \frac{\partial g_1}{\partial x}(x_i, y_i) & x_i \frac{\partial g_1}{\partial y}(x_i, y_i) \\ y_i \frac{\partial g_2}{\partial x}(x_i, y_i) & y_i \frac{\partial g_2}{\partial y}(x_i, y_i) \end{pmatrix} = \begin{pmatrix} J_{11}(E_i) & J_{12}(E_i) \\ J_{21}(E_i) & J_{22}(E_i) \end{pmatrix},
$$

Condition	$E_0(0,0)$	$E_1(1,0)$
$\beta \le \delta$	unstable node	stable node
$\beta > \delta, 0 < h < H_2$	unstable node	saddle
$\beta > \delta, 0 < h = H_2, \beta \ne \widehat{\beta_2}$	unstable node	saddle-node
$\beta > \delta, 0 < h = H_2, \beta = \widehat{\beta_2}$	unstable node	stable node
$\beta > \delta, h > H_2$	unstable node	stable node

Table 2: Summary of the stability of axial equilibria in the case of a weak Allee effect.

implying that

$$J(x_i, y_i) = \begin{pmatrix} x_i \left(\mu + \frac{y_i}{(\alpha+x_i)^2} - 2x_i + 1 \right) & -\frac{x_i}{\alpha+x_i} \\ \frac{\alpha\beta y_i}{(\alpha+x_i)^2} & \frac{hy_i}{(e+y_i)^2} \end{pmatrix}, \tag{14}$$

so that

$$\text{tr}(J_i) = \frac{hy_i}{(e+y_i)^2} + x_i \left(\mu + \frac{y_i}{(\alpha+x_i)^2} - 2x_i + 1 \right), \tag{15}$$

$$\det(J_i) = \frac{hx_iy_i}{(e+y_i)^2} \left(\mu + \frac{y_i}{(\alpha+x_i)^2} - 2x_i + 1 \right) + \frac{\alpha\beta x_iy_i}{(\alpha+x_i)^3}. \tag{16}$$

Therefore, for each of the three internal equilibriums, for elements of the Jacobian matrix J_i we have that $J_{12}(E_i) < 0$, $J_{21}(E_i) > 0$ and $J_{22}(E_i) > 0$. It remain to determine the sign of $J_{11}(E_i)$. Let $\frac{dy^{(g_1)}}{dx}$ and $\frac{dy^{(g_2)}}{dx}$ be gradient of the tangent of curves $g_1(x,y) = 0$ and $g_2(x,y) = 0$, respectively. Then, by using the implicit function theorem, we have

$$J_{11}(E_i) = -x_i \frac{dy^{(g_1)}}{dx}(x_i) \frac{\partial g_1}{\partial y}(x_i, y_i) \tag{17}$$

and we can write the determinant of J_i as

$$\det(J_i) = \left[xy \frac{\partial g_1}{\partial y} \frac{\partial g_2}{\partial y} \left(\frac{dy^{(g_2)}}{dx} - \frac{dy^{(g_1)}}{dx} \right) \right]\Bigg|_{E_i} = J_{12}J_{22} \left[\frac{dy^{(g_2)}}{dx} - \frac{dy^{(g_1)}}{dx} \right]\Bigg|_{E_i}. \tag{18}$$

Considering that $J_{12}(E_i)J_{22}(E_i) < 0$ and $\frac{\partial g_1}{\partial y}(x_i, y_i) < 0$, sign of $\det(J_i)$ and J_{11} depends on gradients of the tangent of predator and prey nontrivial nullclines at the interior equilibrium.

Theorem 3.6. *If an interior equilibrium point $E_2(x_2, y_2)$ exists for some values of parameters, then*

(i) *when*

$$\mu < x_2 \le x_{max} \tag{19}$$

the equilibrium E_2 is an unstable hyperbolic focus or node;

(ii) *when*

$$x_{max} < x_2 < 1 \tag{20}$$

the equilibrium E_2 is
  (a) *a locally unstable point for* $\text{tr}(J_2) > 0$,
  (b) *a locally asymptotic stable point for* $\text{tr}(J_2) < 0$,
  (c) *a weak focus or center for* $\text{tr}(J_2) = 0$.

Proof.   (i) Condition (19) implies that $\frac{dy^{(g_1)}}{dx}(x_2) \geq 0$ (Fig. 4a), which together with (17) imply $J_{11}(E_2) \geq 0$. Then

$$\text{sign}(J_2) = \begin{pmatrix} + & - \\ + & + \end{pmatrix} \quad \vee \quad \text{sign}(J_2) = \begin{pmatrix} 0 & - \\ + & + \end{pmatrix}.$$

Since $\det(J_2) > 0$ and $\text{tr}(J_2) > 0$, the equilibrium E_2 is a locally unstable equilibrium.

(ii) Condition (20) implies that $\frac{dy^{(g_1)}}{dx}(x_2) < 0$ (Fig. 4b), which together with (17) imply $J_{11}(E_2) < 0$. Then

$$\text{sign}(J_2) = \begin{pmatrix} - & - \\ + & + \end{pmatrix}.$$

Considering the slopes of the tangents to the non-trivial prey and predator nullclines at the point E_2, we conclude that $\frac{dy^{(g_1)}}{dx}(x_2) > \frac{dy^{(g_2)}}{dx}(x_2)$, so that (18) gives that $\det(J_2) > 0$. Therefore, stability of the equilibrium E_2 depends on the sign of $\text{tr}(J_2)$. □
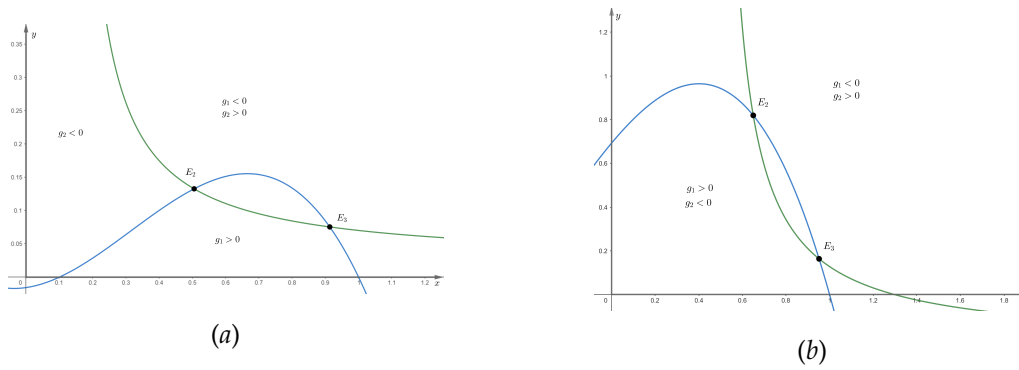

(a) $\qquad\qquad\qquad\qquad\qquad\qquad\qquad\qquad\qquad$ (b)

Figure 4: Stability of the interior equilibria E_2: (a) E_2 is to the left side of the local maximum of $y = \pi_1(x)$, that is $\mu < x_2 \leq x_{max}$; (b) E_2 is on the right side of the local maximum of $y = \pi_1(x)$, that is $x_{max} < x_2 < 1$.

Theorem 3.7. *If the system* (3) *has an interior equilibrium* $E_3(x_3, y_3)$ *for some values of parameters, then* E_3 *is a saddle.*

Proof. Considering the slopes of the tangents to the non-trivial prey and predator nullclines at the point E_3, we conclude that $\frac{dy^{(g_2)}}{dx}(x_3) > \frac{dy^{(g_1)}}{dx}(x_3)$, implying from (18) that $\det(J_3) < 0$. Hence, E_3 is always a saddle. □

For the purpose of the next theorem, we define

$$\begin{aligned}
\vartheta_4 &= \mu - \alpha(\mu + 1) + 3x_4^2 + 2x_4(\alpha - \mu - 1), \\
W_4 &= 2x_4\vartheta_4(1 - x_4)(x_4 - \mu)((\alpha + x_4)^2(1 + \mu - 2x_4) - e) \\
&\quad - (e + y_4)(\alpha + x_4)\Big(x_4^2(-\alpha + 3(x_4 - 2)x_4 + 2) + \mu^2(-\alpha + 2(x_4 - 2)x_4 + 1) \\
&\quad - \mu(\alpha + x_4(-4\alpha + x_4(\alpha + 6x_4 - 12) + 4))\Big),
\end{aligned} \tag{21}$$

where $y_4 = (1 - x_4)(x_4 - \mu)(x_4 + \alpha)$.

Theorem 3.8. *Let $\beta > \delta$ and $h > H_2$. If the equilibrium point $E_4(x_4, y_4)$, $y_4 = (1 - x_4)(x_4 - \mu)(x_4 + \alpha)$ exists for some values of parameters and*

$$\beta = \beta_{BT} = \frac{x_4 \vartheta_4^2 (\alpha + x_4)}{\alpha y_4}, \quad h = h_{BT} = \frac{x_4 \vartheta_4 (e + y_4)^2}{y_4 (\alpha + x_4)} > 0,$$

$$\delta = \delta^\star = \frac{x_4 \vartheta_4 \left((\alpha + x_4)^2 \left(\mu + 3x_4^2 - 2x_4(\mu + 1) \right) - \alpha e \right)}{\alpha y_4 (\alpha + x_4)} > 0, \tag{22}$$

$W_4 \neq 0$, then the interior equilibrium E_4 is a cusp of codimension 2.

Proof. Let $\beta = \beta_{BT}, h = h_{BT}$ and $\delta = \delta^\star$. Conditions $h_{BT} > 0, \delta^\star > 0$ and $\beta_{BT} > \delta^\star$ imply that

$$\vartheta_4 > 0, \quad (\alpha + x_4)^2 (1 + \mu - 2x_4) < e < \frac{(\alpha + x_4)^2 \left(\mu + 3x_4^2 - 2x_4(\mu + 1) \right)}{\alpha}. \tag{23}$$

Conditions (23) imply that $h_{BT} > e\left(\frac{\beta_{BT}}{\alpha + 1} - \delta^\star \right)$ is satisfied. The Jacobian matrix J_4, given by (14), for $(\beta, h, \delta) = (\beta_{BT}, h_{BT}, \delta^\star)$, has two zero eigenvalues, i.e. $\det(J_4) = 0$ and $\operatorname{tr}(J_4) = 0$. In order to discuss the properties of system (3) in the neighborhood of the equilibrium E_4, we translate E_4 to the origin by $X = x - x_4, Y = y - y_4$, expand obtained system in Taylor series, and make the following linear transformation

$$u = -X + \frac{\alpha + x_4}{x_4 \vartheta_4} Y, \quad v = \vartheta_4 X.$$

The obtained system has a form

$$\frac{du}{dt} = v + a_{20}u^2 + a_{11}uv + a_{02}v^2 + O(|(u,v)|^3),$$

$$\frac{dv}{dt} = b_{20}u^2 + b_{11}uv + b_{02}v^2 + O(|(u,v)|^3), \tag{24}$$

where

$$a_{20} = \frac{x_4 \vartheta_4 \left((\alpha + x_4)^2 (1 + \mu - 2x_4) - e \right)}{(\alpha + x_4)^2 (e + y_4)}, \quad a_{11} = \frac{x_4^2 + 2\alpha x_4 - \alpha(\mu + 1) - \mu}{y_4}, \quad a_{02} = -\frac{1}{x_4 \vartheta_4},$$

$$b_{20} = -\frac{x_4^2 \vartheta_4 \left((x_4 + \alpha)^3 (3x_4^2 - 3(\mu + 1)x_4 + \mu^2 + \mu + 1) + e \left(6x_4^2 + 6\alpha x_4 - 3(\mu + 1)x_4 + \alpha^2 - 2\alpha(\mu + 1) + \mu \right) \right)}{(\alpha + x_4)^3 (y_4 + e)},$$

$$b_{11} = -\frac{\left(x_4^2 (2 - \alpha + 3x_4(x_4 - 2)) + \mu^2 (1 - \alpha + 2x_4(x_4 - 2)) - \mu(\alpha(1 + x_4^2) + 4x_4(1 - \alpha) + 6x_4^2(x_4 - 2)) \right)}{y_4},$$

$$b_{02} = \frac{(\alpha - 1)\mu + \alpha - 6x_4^2 + 3x_4(1 - \alpha + \mu)}{x_4 \vartheta_4}.$$

Next, by using the transformation

$$u = \xi + \frac{a_{11} + b_{02}}{2} \xi^2,$$

$$v = \eta - a_{20} \xi^2 + b_{02} \xi \eta - a_{02} \eta^2,$$

the system (24) becomes

$$\frac{d\xi}{dt} = \eta + O(|(\xi, \eta)|^3),$$

$$\frac{d\eta}{dt} = b_{20} \xi^2 + (2a_{20} + b_{11}) \xi \eta + O(|(\xi, \eta)|^3). \tag{25}$$

Using (23) we conclude that $b_{20} \neq 0$ and

$$2a_{20} + b_{11} = \frac{W_4}{y_4(x_4 + \alpha)(e + y_4)} \neq 0.$$

Hence, by Theorem 3. in Section 2.11 of [39], the origin is a cusp of codimension 2 for the system (25), that is, the equilibrium E_4 is a cusp of codimension 2 of the system (3). $\square$

3.3. Uniform persistence

In this section we establish conditions for the uniform persistence of the system (3) in the case of weak Allee effect, using the method of persistence function (or average Lyapunov function), see Gard [19] and Hutson [26]. If a nonlinear system

$$\frac{dx_i}{dt} = x_i f_i(x), \quad i = 1, 2, \dots n \tag{26}$$

is dissipative with corresponding canonical compact $\Pi \subset \mathbb{R}^n_+$, a nonnegative C^1 function $\varrho(x)$ defined on $\overline{\mathbb{R}}^n_+$ is a persistence function for this system, if it satisfies the following two properties:
  (i) $\varrho(x) > 0$, $x \in \mathbb{R}^n_+$ and $\varrho(x) = 0$ for $x \in \partial\mathbb{R}^n_+$
  (ii) $\psi(x) > 0$ for all $x \in \Omega(\partial\mathbb{R}^n_+)$, ω−limit sets of the system in the boundary of the positive cone Π, where

$$\psi(x) = \frac{\dot{\varrho}(x)}{\varrho(x)} = \frac{1}{\varrho(x)} \sum_{k=1}^n \frac{\partial\varrho(x)}{\partial x_k} x_k f_k(x).$$

By Theorem 2 in [19], which is an immediate consequence of Theorem 2.5 in [26], if (26) is dissipative, and if a persistence function ϱ for this system exists, then (26) is uniformly persistent, and hence permanent.

Theorem 3.9. *In the case of weak Allee effect, the system (3) is uniformly persistent if $\beta > \delta$ and $0 < h < H_2$.*

Proof. By Theorem 2.2, solutions of the system (3) with positive initial conditions are uniformly bounded which implies that (3) is dissipative. We will prove uniform persistence of the system (3) by proving that the function $V(x, y) = x^{q_1} y^{q_2}$ where $q_i > 0$, $i = 1, 2$ is a persistence function for the system (3). It holds $V(x, y) > 0$ for all $(x, y) \in \mathbb{R}^2_+$ and $V(x, y) = 0$ if and only if $(x, y) \in \partial\mathbb{R}^2_+$. Under the given conditions, the system has two axial equilibria E_0 and E_1 which are saddles by Theorems 3.3 and 3.4, so they are the only ω-limit sets on axes. We need to check if the function

$$A(x, y) = \frac{\dot{V}(x, y)}{V(x, y)} = \frac{q_1}{x}\frac{dx}{dt} + \frac{q_2}{y}\frac{dy}{dt} = q_1\left((1 - x)(x - \mu) - \frac{y}{\alpha + x}\right) + q_2\left(\frac{\beta x}{\alpha + x} - \delta - \frac{h}{e + y}\right)$$

is positive at E_0 and E_1 for suitable choice of $q_1, q_2 > 0$. We have

$$A(0, 0) = -q_1\mu - q_2\left(\delta + \frac{h}{e}\right), \qquad A(1, 0) = q_2\left(\frac{\beta}{\alpha + 1} - \delta - \frac{h}{e}\right).$$

Since $0 < h < H_2$, then $A(1, 0) > 0$. If we choose $q_1 = -\frac{2}{\mu}(\delta + \frac{h}{e}) > 0$ and $q_2 = 1 > 0$, then $A(0, 0) > 0$. Hence, $V(x, y)$ is a persistence function for the system (3). $\square$

Since the system is dissipative and uniformly persistent under the conditions of Theorem 3.9, it follows that it's uniformly permanent. In biological sense, this guarantees a long time survival of the species.

4. Global stability analysis

4.1. Global stability of trivial equilibrium point $E_0(0,0)$

Theorem 4.1. *In the case of strong Allee effect, if*

$$\beta > \delta \quad and \quad 0 < h \le H_1 = e\left(\frac{\beta\mu}{\alpha+\mu} - \delta\right) \tag{27}$$

the trivial equilibrium point E_0 of the system (3) *is globally asymptotically stable in the first quadrant.*

Proof. If (27) hold, by Theorem 3.1, there is no interior equilibria of the system (3). By Theorem 3.3, the trivial equilibrium E_0 is a locally asymptotically stable. Since $H_1 < H_2$ for $\mu \in (0,1)$, by Theorem 3.4, E_1 is a saddle and by Theorem 3.5, predator-free equilibrium E_μ is an unstable node or repelling saddle-node equilibrium point. All solutions of the system (3) are bounded and eventually end up in the invariant region Ω. Therefore, by using Poincaré–Bendixson theorem, E_0 is globally asymptotically stable in the first quadrant. $\square$

Example 4.2. *For $\mu = 0.5, \alpha = 0.5, \beta = 3.5, \delta = 0.5, e = 0.1, h = 0.1$ the system* (3) *has a globally asymptotically stable trivial equilibrium E_0 (Fig. 5-(a)) since $\mu > 0, \beta > \delta$ and $h \le H_1$.*

4.2. Global stability of predator free equilibrium point $E_1(1,0)$

Theorem 4.3. *In the case of weak Allee effect, if for $h > H_2 = e\left(\frac{\beta}{\alpha+1} - \delta\right)$ there are no interior equilibria, the predator-free equilibrium point E_1 of the system* (3) *is globally asymptotically stable in the first quadrant.*

Proof. If $h > H_2$, by Theorem 3.4, the predator-free equilibrium E_1 is locally asymptotically stable and by Theorem 3.3, the trivial equilibrium E_0 is a saddle. By Theorem 3.2, if $\beta \le \delta$, then the system (3) doesn't have interior equilibria and if $\beta > \delta$ again it is possible that for some values of parameters system doesn't have interior equilibria. All solutions of the system (3) are bounded and eventually end up in the invariant region Ω. Therefore, by using Poincaré–Bendixson theorem, E_1 is globally asymptotically stable in the first quadrant. $\square$

Example 4.4. *For $\mu = -0.5, \alpha = 1, \beta = 1.1, \delta = 0.3, e = 0.4, h = 0.25$ the system* (3) *has a globally asymptotic stable predator-free equilibrium E_1 (Fig. 5-(b)) since $\mu < 0$ and $h > H_2$.*

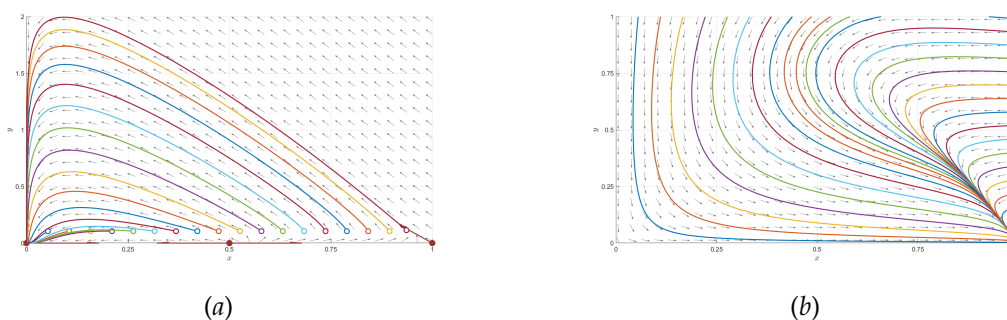(a)   (b)

Figure 5: (a) Phase portrait of the system (3) for $\mu = 0.5, \alpha = 0.5, \beta = 3.5, \delta = 0.5, e = 0.1, h = 0.1$. Trivial equilibrium E_0 is globally asymptotically stable. (b) Phase portrait of the system (3) for $\mu = -0.5, \alpha = 1, \beta = 1.1, \delta = 0.3, e = 0.4, h = 0.25$. The predator-free equilibrium E_1 is globally asymptotic stable.

5. Bifurcation analysis

This section is dedicated to examination of the possible bifurcation at the equilibrium points of the system (3), when the parameter values are varied.

5.1. Transcritical and pitchfork bifurcations

We use Sotomayor's theorem [39] to prove that the system (3) undergoes a transcritical and pitchfork bifurcation around some equilibrium point. To simplify notation, we write the system (3) in the vector form

$$(x', y')^T = F(x, y) = (F_1(x, y), F_2(x, y))^T = (xg_1(x, y), yg_2(x, y))^T,$$

and we have that

$$F_h = \left(\frac{\partial F_1}{\partial h}, \frac{\partial F_2}{\partial h}\right)^T.$$

For $G = (G_1, G_2) \in C^3(E)$, $E \subset \mathbb{R}^2$ and $v = (v_1, v_2) \in \mathbb{R}^2$, we define operators

$$D^2 G(x, y)(v, v) = \begin{pmatrix} \frac{\partial^2 G_1}{\partial x^2} v_1^2 + 2\frac{\partial^2 G_1}{\partial x \partial y} v_1 v_2 + \frac{\partial^2 G_1}{\partial y^2} v_2^2 \\ \frac{\partial^2 G_2}{\partial x^2} v_1^2 + 2\frac{\partial^2 G_2}{\partial x \partial y} v_1 v_2 + \frac{\partial^2 G_2}{\partial y^2} v_2^2 \end{pmatrix}_{(x,y)},$$

$$D^3 G(x, y)(v, v, v) = \begin{pmatrix} \frac{\partial^3 G_1}{\partial x^3} v_1^3 + 3\frac{\partial^3 G_1}{\partial x^2 \partial y} v_1^2 v_2 + 3\frac{\partial^3 G_1}{\partial x \partial y^2} v_1 v_2^2 + \frac{\partial^3 G_1}{\partial y^3} v_2^3 \\ \frac{\partial^3 G_2}{\partial x^3} v_1^3 + 3\frac{\partial^3 G_2}{\partial x^2 \partial y} v_1^2 v_2 + 3\frac{\partial^3 G_2}{\partial x \partial y^2} v_1 v_2^2 + \frac{\partial^3 G_2}{\partial y^3} v_2^3 \end{pmatrix}_{(x,y)}.$$

In Section 3.2, we concluded that the equilibrium E_μ is an unstable node for $h < H_1$. It becomes a hyperbolic saddle for $h > H_1$ and the interior equilibrium E_2 appears. For $h = H_1$, E_μ coincides with an interior equilibrium E_2. Therefore, we will examine the existence of transcritical bifurcation at the equilibrium E_μ by taking h as bifurcation parameter. Through a transcritical bifurcation, an unstable interior equilibrium E_2 becomes a biologically feasible when h crosses the transcritical bifurcation threshold $h = H_1 > 0$.

Theorem 5.1. *Let $0 < \mu < 1$, $\beta > \delta$. System (3) undergoes a transcritical bifurcation at the equilibrium E_μ for the critical value $h = h_{TC_1} = H_1 > 0$.*

Proof. The Jacobian matrix at the equilibrium E_μ for the critical value $h = h_{TC_1}$ is

$$J_{h_{TC_1}} = J(E_\mu)\big|_{h=h_{TC_1}} = \begin{pmatrix} (1-\mu)\mu & -\frac{\mu}{\alpha+\mu} \\ 0 & 0 \end{pmatrix}.$$

We find that $\det(J_{h_{TC_1}}) = 0$, that is one of the eigenvalue of $J_{h_{TC_1}}$ is zero, with the corresponding eigenvector $V = \left(\frac{1}{(1-\mu)(\alpha+\mu)}, 1\right)^T$. The eigenvector corresponding to zero eigenvalue of the matrix $J_{h_{TC_1}}^T$ is $W = (0, 1)^T$. We check the transversality conditions for transcritical bifurcation according to the Sotomayor's theorem. We have

$$F_h(E_\mu)\big|_{h=h_{TC_1}} = (0, 0)^T,$$

$$\Delta_1 = W^T\left(F_h(E_\mu)\big|_{h=h_{TC_1}}\right) = 0,$$

$$\Delta_2 = W^T\left(DF_h(E_\mu)\big|_{h=h_{TC_1}}\right)V = -\frac{1}{e} \neq 0,$$

$$\Delta_3 = W^T\left(D^2 F(E_\mu)(V, V)\big|_{h=h_{TC_1}}\right) = \frac{2(e\alpha\beta + (1-\mu)(\alpha+\mu)^2(\beta\mu - \delta(\alpha+\mu)))}{e(1-\mu)(\alpha+\mu)^3}.$$

Since the condition $H_1 > 0$ implies $\beta\mu - \delta(\alpha + \mu) > 0$, we have that $\Delta_3 > 0$, so that the transversality conditions for the transcritical bifurcation are satisfied. By using Sotomayor's theorem, we conclude that the system (3) experience a transcritical bifurcation around the equilibrium E_μ at the bifurcation threshold $h = h_{TC_1} = H_1$. $\square$

An equilibrium E_1 is a saddle for $h < H_2$, and a stable node for $h > H_2$. If $h > H_2$, the interior equilibrium E_3 exists for some values of parameters and it is a saddle whenever exists. When $h = H_2 > 0$, E_1 collides with the interior equilibrium E_3. In the following theorem, we will examine the conditions under which the system (3) undergoes transcritical bifurcation at the equilibrium E_1 when the parameter h crosses the bifurcation threshold $h = h_{TC_2} = H_2 > 0$. We will show that an interior equilibrium E_3 bifurcates from E_1 when h passes over that threshold (Fig. 6).
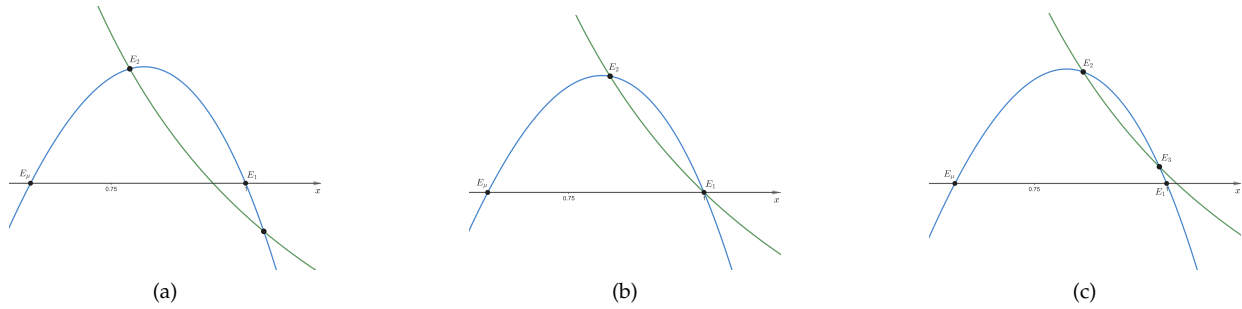

(a) (b) (c)

Figure 6: Transcritical bifurcation at $E_1(1,0)$ at the bifurcation threshold $h = h_{TC_2} = H_2$, for $\beta \neq \widehat{\beta_2}$; (a) For $h < h_{TC_2}$: an unique interior equilibrium E_2 exists and E_1 is a saddle. (b) E_1 is saddle-node for $h = h_{TC_2}$ and $\beta \neq \widehat{\beta_2}$; (c) For $h > h_{TC_2}$: E_1 is stable node and the interior equilibrium E_3 appears, which is a saddle.

Theorem 5.2. *Let $\beta > \delta$ and $\beta \neq \widehat{\beta_2}$, $\widehat{\beta_2}$ given by (10). System (3) undergoes a transcritical bifurcation at the equilibrium E_1 for the critical value $h = h_{TC_2} = H_2 > 0$.*

Proof. The Jacobian matrix at the equilibrium E_1 for the critical value $h = h_{TC_2}$ is

$$J_{h_{TC_2}} = J(E_1)\big|_{h=h_{TC_2}} = \begin{pmatrix} \mu - 1 & -\frac{1}{\alpha+1} \\ 0 & 0 \end{pmatrix}.$$

We find that $\det(J_{h_{TC_2}}) = 0$, that is one of the eigenvalue of $J_{h_{TC_2}}$ is zero, with the corresponding eigenvector $V = \left(\frac{1}{(\alpha+1)(\mu-1)}, 1\right)^T$. The eigenvector corresponding to zero eigenvalue of the matrix $J_{h_{TC_2}}^T$ is $W = (0,1)^T$. We check the transversality conditions for transcritical bifurcation according to the Sotomayor's theorem. We have

$$F_h(E_1)\big|_{h=h_{TC_2}} = (0,0)^T$$

$$\Delta_1 = W^T\left(F_h(E_1)\big|_{h=h_{TC_2}}\right) = 0,$$

$$\Delta_2 = W^T\left(DF_h(E_1)\big|_{h=h_{TC_2}}\right)V = -\frac{1}{e} \neq 0,$$

$$\Delta_3 = W^T\left(D^2F(E_1)(V,V)\big|_{h=h_{TC_2}}\right) = 2\frac{(\mu-1)(\alpha+1)^2(\beta - \delta(\alpha+1)) + e\alpha\beta}{(\alpha+1)^3 e(\mu-1)}.$$

Then, $\Delta_3 \neq 0$ for $\beta \neq \widehat{\beta_2}$. Therefore, by using Sotomayor's theorem, we obtain that system (3) undergoes a transcritical bifurcation at the equilibrium E_1 for the critical value $h = h_{TC_2}$. $\square$

If $\beta = \widehat{\beta_2} > 0$ we will show that through a pitchfork bifurcation at E_1, the interior equilibrium E_2 disappears when h crosses the pitchfork bifurcation threshold $h = h_{PC} = H_2 > 0$. In fact, an unique interior equilibrium E_2 exists for $H_1 < h < H_2$ and it collides with E_1 for $h = H_2$ if $\beta = \widehat{\beta_2} > 0$ and for $h > H_2$ if $\beta = \widehat{\beta_2} > 0$ there is no interior equilibria of the system (Fig. 7). Note that by Theorem 3.4, for $h = H_2$ if $\beta = \widehat{\beta_2} > 0$, the predator free equilibrium E_1 is a stable node.

Theorem 5.3. *Let $\beta > \delta$ and $\beta = \widehat{\beta_2} > 0$. System* (3) *undergoes a pichfork bifurcation at the equilibrium E_1 for the critical value $h = h_{PC} = H_2 > 0$.*

Proof. From the proof of the Theorem 5.2, for $\beta = \widehat{\beta_2} > 0$ we have that $\Delta_3 = 0$ and

$$\Delta_4 = W^T \left(D^3 F(E_1)(V, V, V) \big|_{h=h_{PC}} \right) = \frac{6\alpha\delta \left((\alpha+1)^2 (1-\mu) + e \right)}{(\alpha+1)^2 e (1-\mu)(e\alpha + (\alpha+1)^2(\mu-1))} \neq 0, .$$

By using Sotomayor's theorem, we conclude that system (3) undergoes a pitchfork bifurcation at the equilibrium E_1 for the critical value $h = h_{PC}$. $\square$
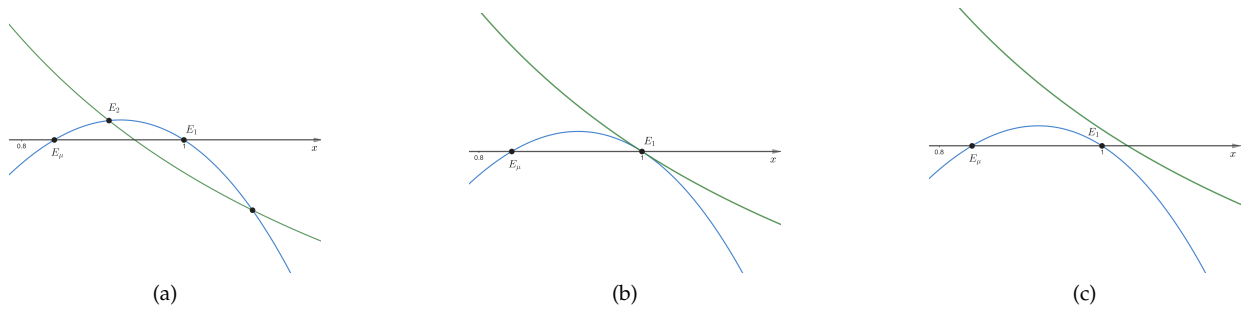

(a)   (b)   (c)

Figure 7: Pitchfork bifurcation at $E_1(1,0)$ at the bifurcation threshold $h = h_{PC} = H_2$, for $\beta = \widehat{\beta_2}$; (*a*) For $h < h_{PC}$: E_1 is a saddle and an unique interior equilibrium E_2 exists; (*b*) For $h = h_{PC}$: E_2 collides with E_1 and E_1 is a stable node; (*c*) For $h > h_{PC}$: E_1 is a stable node and an unique interior equilibrium E_2 disappears.

5.2. Hopf bifurcation

In Theorems 3.6 and 3.7 it was shown that interior equilibrium E_3 is always a saddle, while the stability of E_2 can be changed. In the following theorem, we will show that the stability of E_2 is changed through a Hopf bifurcation.

Theorem 5.4. *Let $\beta > \delta$, $h > H_1$ and suppose that the interior equilibrium E_2 exists for some values of parameters. The interior equilibrium E_2 changes its stability through Hopf bifurcation at the threshold $h = h_H > H_1$, if*

$$(i) \ \ tr(J_2)\big|_{h=h_H} = 0, \qquad (ii) \ \ \frac{d}{dh} \left(tr(J_2) \right) \big|_{h=h_H} \neq 0 . \tag{28}$$

Proof. According to the proof of Theorem 3.6, $\det(J_2) > 0$. If (28)-(i) is satisfied, the matrix J_2 has a pair of purely imaginary eigenvalues for $h = h_H$. Moreover, if (28)-(ii) holds, the transversality conditions for Hopf bifurcation will be satisfied. Hence, by using Poincare–Andronov Hopf bifurcation theorem [46], the system (3) undergoes Hopf bifurcation around E_2 at the critical value $h = h_H$. $\square$

In order to identify direction of Hopf bifurcation we need to compute the first Lyapunov coefficient. Applying translation $x = X + x_2$, $y = Y + y_2 = Y + (1-x_2)(x_2+\alpha)(x_2-\mu)$, the point E_2 is transformed to the origin and expanding in Taylor series around $(0,0)$ obtained system, the system (3) takes the form

$$\begin{aligned}
\frac{dX}{dt} &= a_{10}X + a_{01}Y + a_{20}X^2 + a_{11}XY + a_{30}X^3 + a_{21}X^2Y + \phi_1(X,Y), \\
\frac{dY}{dt} &= b_{10}X + b_{01}Y + b_{20}X^2 + b_{11}XY + b_{02}Y^2 + b_{30}X^3 + b_{21}X^2Y + b_{03}Y^3 + \phi_2(X,Y),
\end{aligned} \tag{29}$$

where

$$a_{10} = x_2\left(2(\mu+1) - 3x_2\right) - \mu - \frac{\alpha y_2}{(\alpha + x_2)^2}, \quad a_{01} = -\frac{x_2}{\alpha + x_2}, \quad a_{20} = 1 + \mu - 3x_2 + \frac{\alpha y_2}{(\alpha + x_2)^3},$$

$$a_{11} = -\frac{\alpha}{(\alpha + x_2)^2}, \quad a_{30} = -\frac{\alpha y_2}{(\alpha + x_2)^4} - 1, \quad a_{21} = \frac{\alpha}{(\alpha + x_2)^3},$$

$$b_{10} = \frac{\alpha\beta y_2}{(\alpha + x_2)^2}, \quad b_{01} = -\delta - \frac{eh}{(e + y_2)^2} + \frac{\beta x_2}{\alpha + x_2}, \quad b_{20} = -\frac{\alpha\beta y_2}{(\alpha + x_2)^3}, \quad b_{11} = \frac{\alpha\beta}{(\alpha + x_2)^2},$$

$$b_{02} = \frac{eh}{(e + y_2)^3}, \quad b_{30} = \frac{\alpha\beta y_2}{(\alpha + x_2)^4}, \quad b_{21} = -\frac{\alpha\beta}{(\alpha + x_2)^3}, \quad b_{03} = -\frac{eh}{(e + y_2)^4},$$

and $\phi_1(X, Y)$ and $\phi_2(X, Y)$ are smooth functions of X and Y at least of order four. The first Lyapunov number [39] is calculated by

$$\begin{aligned}
\sigma = \frac{-3\pi}{2a_{01}\omega_0^{3/2}} &\Big(\big((a_{10}b_{10}(a_{11}^2 + a_{11}b_{02} + a_{02}b_{11}) + a_{10}a_{01}(b_{11}^2 + a_{20}b_{11} + a_{11}b_{02})\big) \\
&+ b_{10}^2(a_{11}a_{02} + 2a_{02}b_{02}) - 2a_{10}b_{10}(b_{02}^2 - a_{20}a_{02}) - 2a_{10}a_{01}(a_{20}^2 - b_{20}b_{02}) \\
&- a_{01}^2(2a_{20}b_{20} + b_{11}b_{20}) + (a_{01}b_{10} - 2a_{10}^2)(b_{11}b_{02} - a_{11}a_{20})\big) \\
&- (a_{10}^2 + a_{01}b_{10})\left(3(b_{10}b_{03} - a_{01}a_{30}) + 2a_{10}(a_{21} + b_{12}) + (b_{10}a_{12} - a_{01}b_{21})\right)\Big)\Big|_{h=h_{\mathrm{H}}},
\end{aligned}$$

where $\omega_0 = \det(J_2)$. Since the expression of the first Lyapunov number σ is quite complicated, conditions for parameters under which sign of the first Lyapunov coefficient can change, are very difficult to obtain. The following statements hold:

 (i) if $\sigma < 0$ then the system (3) undergoes the supercritical Hopf bifurcation.
 (ii) if $\sigma > 0$ then the system (3) undergoes the subcritical Hopf bifurcation.
 (iii) if $\sigma = 0$ then the system (3) undergoes the degenerate Hopf bifurcation.

We are unable to give the exact analytical expression for h_H as we do not have the explicit form of the interior equilibrium point E_2, but numerically we show that the system undergoes supercritical Hopf bifurcation in the case of strong Allee effect as well as in the case of weak Allee effect.

5.3. Bogdanov-Takens bifurcation

A dynamical system undergoes a Bogdanov-Takens (BT) bifurcation at an equilibrium point whenever the Jacobian matrix at that equilibrium point has a zero eigenvalue of multiplicity two. Under the conditions of Theorem 3.8, the interior equilibrium $E_4(x_4, x_4(1 - x_4)(x_4 - \mu))$ is cusp of codimension 2. In the following theorem we will prove that the Bogdanov-Takens bifurcation will occur in the system (3) in the small neighborhood of the equilibrium E_4, taking β and h as Bogdanov-Takens bifurcation parameters. Denote with

$$\begin{aligned}
Z_4 = \frac{x_4}{(e + y_4)^5(\alpha + x_4)^7}&\Big(x_4 y_4(e + y_4)\big(-y_4(\alpha + x_4)\big(2\big(\mu(\alpha + x_4)^3 - 3x_4(\alpha + x_4)^3 \\
&+ (\alpha + x_4)^3 + \alpha y_4\big)\big(eh_{\mathrm{BT}}(\alpha + x_4) + \delta^\star(e + y_4)^2(\alpha + x_4) + \beta_{\mathrm{BT}}(-x_4)(e + y_4)^2\big) + \alpha\beta_{\mathrm{BT}}(e + y_4)^2\big(\mu(\alpha + x_4)^2 \\
&+ x_4(\alpha + x_4)^2(3x_4 - 2(\mu + 1)) + \alpha y_4\big) + 2\alpha\beta_{\mathrm{BT}}x_4 y_4(e + y_4)^2 + \alpha^2\beta_{\mathrm{BT}}(-y_4)(e + y_4)^2\big) + (e + y_4)^2(\alpha + x_4)^2(x_4(2\mu - 3x_4 \\
&+ 2) - \mu)\big(\alpha\beta_{\mathrm{BT}}e(\alpha + x_4) + (e + y_4)\big(-2(\mu + 1)(\alpha + x_4)^3 + 6x_4(\alpha + x_4)^3 - \alpha(\beta_{\mathrm{BT}}(\alpha + x_4) + 2y_4)\big)\big) \\
&+ e(e + y_4)^2\big(-2(\mu + 1)(\alpha + x_4)^3 + 6x_4(\alpha + x_4)^3 - 2\alpha y_4\big)\big(\mu(\alpha + x_4)^2 + x_4(\alpha + x_4)^2(3x_4 - 2(\mu + 1)) + \alpha y_4\big)\big) \\
&- \big(\mu(\alpha + x_4)^2 + x_4(\alpha + x_4)^2(3x_4 - 2(\mu + 1)) + \alpha y_4\big)\big(y_4^2(\alpha + x_4)\big(\alpha(e + y_4)\big(eh_{\mathrm{BT}}(\alpha + x_4) + \delta^\star(e + y_4)^2(\alpha + x_4) \\
&+ \beta_{\mathrm{BT}}(-x_4)(e + y_4)^2\big) - 2eh_{\mathrm{BT}}(\alpha + x_4)\big(\mu(\alpha + x_4)^2 + x_4(\alpha + x_4)^2(3x_4 - 2(\mu + 1)) + \alpha y_4\big) + \alpha\beta_{\mathrm{BT}}x_4(e + y_4)^3\big)
\end{aligned}$$

$$+ (e + y_4)(\alpha + x_4)^2 (x_4(2\mu - 3x_4 + 2) - \mu)\Big(y_4\big(\alpha(e + y_4)^3 - 2eh_{BT}(\alpha + x_4)^2\big) - e(\alpha + x_4)\big(eh_{BT}(\alpha + x_4)$$

$$+ \delta^\star(e + y_4)^2(\alpha + x_4) + \beta_{BT}(-x_4)(e + y_4)^2\big)\big) + e\big(\mu(\alpha + x_4)^2 + x_4(\alpha + x_4)^2(3x_4 - 2(\mu + 1)) + \alpha y_4\big(y_4\big(\alpha(e + y_4)^3$$

$$- 2eh_{BT}(\alpha + x_4)^2\big) - (e + y_4)(\alpha + x_4)\big(eh_{BT}(\alpha + x_4) + \delta^\star(e + y_4)^2(\alpha + x_4) + \beta_{BT}(-x_4)(e + y_4)^2\big)\big)\big)\big),$$

where $y_4 = (1 - x_4)(x_4 - \mu)(x_4 + \alpha)$ and $\beta_{BT}, h_{BT}, \delta_*$ are given by (22).

Theorem 5.5. *Let $\beta > \delta, h > H_2$ and the equilibrium E_4 exists for some values of parameters. If $h_{BT} > 0, \delta = \delta_* > 0, W_4 \neq 0$ and $Z_4 \neq 0$ where $\beta_{BT}, h_{BT}, \delta_*$ are given by (22) and W_4 is given by (21), then system (3) undergoes Bogdanov-Takens bifurcation around the equilibrium E_4, when (β, h) is varied near (β_{BT}, h_{BT}).*

Proof. To show that the system (3) undergoes the Bogdanov-Takens bifurcation when (β, h) varies in the neighborhood of (β_{BT}, h_{BT}), we consider the unfolding system of the system (3)

$$\frac{dx}{dt} = x(1 - x)(x - \mu) - \frac{xy}{\alpha + x},$$
$$\frac{dy}{dt} = \frac{(\beta_{BT} + \lambda_1)xy}{\alpha + x} - \delta_* y - \frac{(h_{BT} + \lambda_2)y}{e + y}, \tag{30}$$

where $\lambda = (\lambda_1, \lambda_2) = (\beta - \beta_{BT}, h - h_{BT})$ is a parameter vector varying in a small neighbourhood of $(0, 0)$. We reduce the system (30) in the normal form of a Bogdanov–Takens bifurcation, by employing a series of change of coordinates in a small neighborhood of the origin. First apply the linear transformation $u = x - x_4, v = y - x_4(1 - x_4)(x_4 - \mu)$ and then we expand the obtained system in Taylor series around the point $(0, 0)$ to obtain the system

$$\frac{du}{dt} = p_1(u, v, \lambda) = a_{00} + a_{10}u + a_{01}v + a_{20}u^2 + a_{11}uv + a_{02}v^2 + R_1(u, v, \lambda),$$
$$\frac{dv}{dt} = p_2(u, v, \lambda) = b_{00} + b_{10}u + b_{01}v + b_{20}u^2 + b_{11}uv + b_{02}v^2 + R_2(u, v, \lambda), \tag{31}$$

where

$$a_{00} = 0, \quad a_{10} = -\frac{x_4 \vartheta_4}{\alpha + x_4}, \quad a_{01} = -\frac{x_4}{\alpha + x_4}, \quad a_{20} = \mu + \frac{\alpha y_4}{(\alpha + x_4)^3} - 3x_4 + 1, \quad a_{11} = -\frac{\alpha}{(\alpha + x_4)^2}, \quad a_{02} = 0,$$

$$b_{00} = -\frac{y_4(h_{BT} + \lambda_2)}{e + y_4} + \frac{x_4 y_4(\beta_{BT} + \lambda_1)}{\alpha + x_4} - \delta_* y_4, \quad b_{10} = \frac{\alpha y_4(\beta_{BT} + \lambda_1)}{(\alpha + x_4)^2}, \quad b_{20} = -\frac{\alpha y_4(\beta_{BT} + \lambda_1)}{(\alpha + x_4)^3},$$

$$b_{01} = -\frac{e(h_{BT} + \lambda_2)}{(e + y_4)^2} + \frac{x_4(\beta_{BT} + \lambda_1)}{\alpha + x_4} - \delta_*, \quad b_{11} = \frac{\alpha(\beta_{BT} + \lambda_1)}{(\alpha + x_4)^2}, \quad b_{02} = \frac{e(h_{BT} + \lambda_2)}{(e + y_4)^3},$$

and $R_1(u, v, \lambda), R_2(u, v, \lambda)$ are at least of the third order with terms $u^i v^j$, whose coefficients depend smoothly on $\lambda = (\lambda_1, \lambda_2)$. Next, since $a_{01} \neq 0$, we apply variable transformation and time reparametrization near the origin

$$X = u, \quad Y = \frac{du}{dt}, \quad dt = \left(1 - \frac{a_{11} + b_{02}}{a_{01}}X\right)d\tau,$$

and obtain

$$\frac{dX}{d\tau} = Y,$$
$$\frac{dY}{d\tau} = c_{00} + c_{10}X + c_{01}Y + c_{20}X^2 + c_{11}XY + R_3(X, Y, \lambda), \tag{32}$$

where $R_3(X, Y, \lambda)$ is at least of the third order with terms $X^i Y^j$, whose coefficients depend smoothly on $\lambda = (\lambda_1, \lambda_2)$ and

$$c_{00} = a_{01}b_{00}, \quad c_{10} = -a_{10}b_{01} - b_{00}(a_{11} + 2b_{02}) + a_{01}b_{10}, \quad c_{01} = a_{10} + b_{01},$$

$$c_{20} = \frac{-a_{11}^2 b_{00} + b_{02}(a_{10}^2 + 2a_{10}b_{01} + b_{00}b_{02}) + a_{11}(2a_{10}b_{01} - a_{01}b_{10}) - a_{01}(a_{20}b_{01} + 2b_{02}b_{10} + a_{10}b_{11}) + a_{01}^2 b_{20}}{a_{01}},$$

$$c_{11} = 2a_{20} + b_{11} - \frac{2a_{10}a_{11} + a_{11}b_{01} + 3a_{10}b_{02} + b_{01}b_{02}}{a_{01}}.$$

The direction of time is preserved near the origin for small λ. We have

$$c_{20}\big|_{\lambda=0} = \frac{x_4^2 \vartheta_4}{(\alpha + x_4)^3 (y_4 + e)} \Big(e \big(\alpha^2 - 2\alpha(\mu + 1) + \mu + 6x_4^2 + 6\alpha x_4 - 3(\mu + 1)x_4 \big)$$

$$+ (\alpha + x_4)^3 \left(\mu^2 + \mu + 3x_4^2 - 3(\mu + 1)x_4 + 1 \right) \Big) > 0$$

under the conditions (23). Also

$$c_{11}\big|_{\lambda=0} = -\frac{W_4}{y_4(e + y_4)(x_4 + \alpha)} \neq 0.$$

Finally, making the following variable substitutions

$$x_1 = X + \frac{c_{01}}{c_{11}}, \quad y_1 = Y,$$

$$x_2 = \frac{c_{11}^2}{c_{20}} x_1, \quad y_2 = \frac{c_{11}^3}{c_{20}^2} y_1, \quad ds = \frac{c_{20}}{c_{11}} d\tau \tag{33}$$

we obtain a versal unfolding form of the system (3)

$$\frac{dx_2}{ds} = y_2,$$

$$\frac{dy_2}{ds} = \mu_1 + \mu_2 x_2 + x_2^2 + x_2 y_2 + R_4(x_2, y_2, \lambda), \tag{34}$$

where $R_4(x_2, y_2, \lambda)$ is at least of the third order with terms $x_2^i y_2^j$, whose coefficients depend smoothly on $\lambda = (\lambda_1, \lambda_2)$ and

$$\mu_1 = \frac{-c_{01}c_{10}c_{11}^3 + c_{00}c_{11}^4 + c_{01}^2 c_{11}^2 c_{20}}{c_{20}^3}, \quad \mu_2 = \frac{c_{10}c_{11}^2 - 2c_{01}c_{11}c_{20}}{c_{20}^2}.$$

Observe the map:

$$(u, v, \lambda_1, \lambda_2) \rightarrow (p(u, v, \lambda), \operatorname{tr}(A(u, v)), \det(A(u, v))),$$

where $p(u, v, \lambda) = (p_1(u, v, \lambda), p_2(u, v, \lambda))$ is a vector field of the system (31) and $A = \frac{\partial(p_1, p_2)}{\partial(u, v)}$. By using Lema 8.6 in [30], the transversality condition for Bogdanov-Takens bifurcation is equivalent to the regularity of this map at $(0, 0, 0, 0)$. This is satisfied since

$$\left| \frac{\partial(p_1, p_2, \operatorname{tr}(A), \det(A))}{\partial(u, v, \lambda_1, \lambda_2)} \right|_{(u,v)=(0,0), \lambda=0} = Z_4 \neq 0.$$

Hence, from [5, 6, 44] and Theorem 8.4 in [30], it follows that the system (34) (and (30)) undergoes Bogdanov-Takens bifurcation when (λ_1, λ_2) varies in a small neighbourhood of $(0, 0)$. $\square$

In the previous proof, we used the time reparametrization $ds = \frac{c_{20}}{c_{11}} d\tau$ in (33) to obtain the system (34). Since, $\text{sign}\left(\frac{c_{20}}{c_{11}}\Big|_{\lambda=0}\right) = -\text{sign}(W_4)$ we conclude:

1. if $W_4 > 0$ then $\frac{c_{20}}{c_{11}}\Big|_{\lambda=0} < 0$. Therefore, the system (3) undergoes Bogdanov-Takens bifurcation around E_4 which includes saddle-node bifurcation, supercritical Hopf bifurcation and homoclinic bifurcation, when (β, h) is varied near (β_{BT}, h_{BT}).

2. if $W_4 < 0$ then $\frac{c_{20}}{c_{11}}\Big|_{\lambda=0} > 0$. Therefore, the system (3) undergoes Bogdanov-Takens bifurcation around E_4 which includes saddle-node bifurcation, subcritical Hopf bifurcation and homoclinic bifurcation, when (β, h) is varied near (β_{BT}, h_{BT}).

The bifurcation curves can be locally represented (see [30]) as

(i) Saddle-node bifurcation curves:

$$SN^- = \{(\lambda_1, \lambda_2) : 4\mu_1(\lambda_1, \lambda_2) - \mu_2^2(\lambda_1, \lambda_2) = 0, \mu_2(\lambda_1, \lambda_2) < 0\}$$
$$SN^+ = \{(\lambda_1, \lambda_2) : 4\mu_1(\lambda_1, \lambda_2) - \mu_2^2(\lambda_1, \lambda_2) = 0, \mu_2(\lambda_1, \lambda_2) > 0\}$$

(ii) Hopf bifurcation curve: $H = \{(\lambda_1, \lambda_2) : \mu_1(\lambda_1, \lambda_2) = 0, \mu_2(\lambda_1, \lambda_2) < 0\}$;

(iii) Homoclinic bifurcation curve:
$$HL = \left\{(\lambda_1, \lambda_2) : \mu_1(\lambda_1, \lambda_2) = -\frac{6}{25}\mu_2^2(\lambda_1, \lambda_2), \mu_2(\lambda_1, \lambda_2) < 0\right\}.$$

6. Numerical simulation

In this section, we perform numerical simulations to validate our analytical findings from the previous sections. First, we demonstrate that the system undergoes a supercritical Hopf bifurcation in both the cases of strong Allee effect and weak Allee effect considering h as the bifurcation parameter.
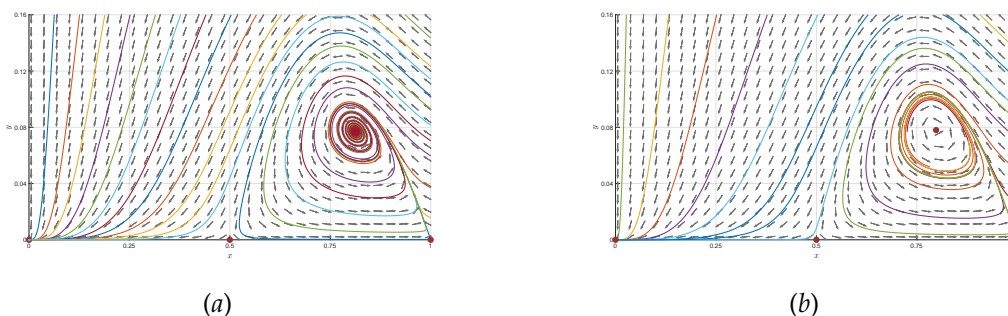

(a) $\qquad\qquad\qquad\qquad\qquad\qquad\qquad\qquad (b)$

Figure 8: Phase portraits of the system (3) for $\mu = 0.5, \alpha = 0.5, \beta = 2.8, \delta = 1.62, e = 0.1$ and parameter h is varied; (a) Interior equilibria E_2 is stable, for $h = 0.02$; (b) Existence of stable limit cycle enclosing an unstable hyperbolic focus, for $h = 0.018$. Stability of equilibrium points corresponding to these phase portraits is summarized in Table 3.

Example 6.1. *Let us fix parameters $\mu = 0.5, \alpha = 0.5, \beta = 2.8, \delta = 1.62, e = 0.1$. A system (3) has three axial equilibria: a stable node E_0, a saddle $E_\mu(0.5, 0)$, and $E_1(1, 0)$ which can change stability. Since $H_1 = -0.022$, a system has one interior equilibrium E_2 and E_1 is a saddle for $0 < h < H_2 = 0.0247$. A Hopf bifurcation threshold value is $h_H = 0.018555$. For $h = h_H$, the equilibrium $E_2(0.801485, 0.077893)$ is a stable weak focus of multiplicity one, and since the first Lyapunov number is $\sigma = -174.602 < 0$, the system undergoes a supercritical Hopf bifurcation at E_2. Because of transversality condition $\frac{d}{dh}(\text{tr}(J_2)) = -10.1527 < 0$, an unique stable limit cycle bifurcates from E_2 as h decreases from bifurcation threshold h_H.*

- *For $h = 0.02 > h_H$ a system (3) has one interior equilibrium $E_2(0.812127, 0.0769434)$ which is a stable focus and there is no closed orbits. (Fig. 8-(a)).*

- *For $h = 0.018 < h_H$ a system (3) has one interior equilibrium $E_2(0.797534, 0.0781641)$ which is an unstable equilibrium surrounded by a stable limit cycle. (Fig. 8-(b)).*

h	Equilibria	Eigenvalues		Stability	Remark
		Re(λ_1)	Re(λ_2)		
0.02	$E_0(0,0)$	−1.82	−0.5	stable	bi-stable
	$E_1(1,0)$	−0.5	0.04667	saddle	
	$E_\mu(0.5,0)$	−0.42	0.25	saddle	
	$E_2(0.81213, 0.07694)$	−0.00773	−0.00773	stable	
0.018	$E_0(0,0)$	−1.8	−0.5	stable	bi-stable
	$E_1(1,0)$	−0.5	0.06667	saddle	Stable cycle
	$E_\mu(0.5,0)$	−0.4	0.25	saddle	around E_2
	$E_2(0.79753, 0.07816)$	0.00277	0.00277	unstable	

Table 3: Summary of the stabilty of equilibrium points corresponding to the phase portraits presented in Figure 8.

Example 6.2. *Let us fix parameters $\mu = -0.3, \alpha = 0.5, \beta = 2, \delta = 0.94, e = 0.3$. A system (3) has two axial equilibria: an unstable node E_0 and $E_1(1,0)$ which can change stability. A system has one interior equilibrium E_2 and E_1 is a saddle for $0 < h < H_2 = 0.118$. A Hopf bifurcation threshold value is $h_H = 0.0975301$. For $h = h_H$, the equilibrium $E_2(0.586573, 0.398265)$ is a stable weak focus of multiplicity one, and since the first Lyapunov number is $\sigma = -63.7884 < 0$, the system undergoes a supercritical Hopf bifurcation at E_2. Because of transversality condition $\frac{d}{dh}(\text{tr}(J_2)) = -2.23552 < 0$, an unique stable limit cycle bifurcates from E_2 as h decreases from bifurcation threshold h_H.*

- *For $h = 0.11 > h_H$ a system (3) has one interior equilibrium $E_2(0.609234, 0.394108)$ which is a stable focus and there is no closed orbits. (Fig. 9-(a)).*

- *For $h = 0.08 < h_H$ a system (3) has one interior equilibrium $E_2(0.557168, 0.401281)$ which is an unstable equilibrium surrounded by a stable limit cycle. (Fig. 9-(b)).*

(a)   (b)
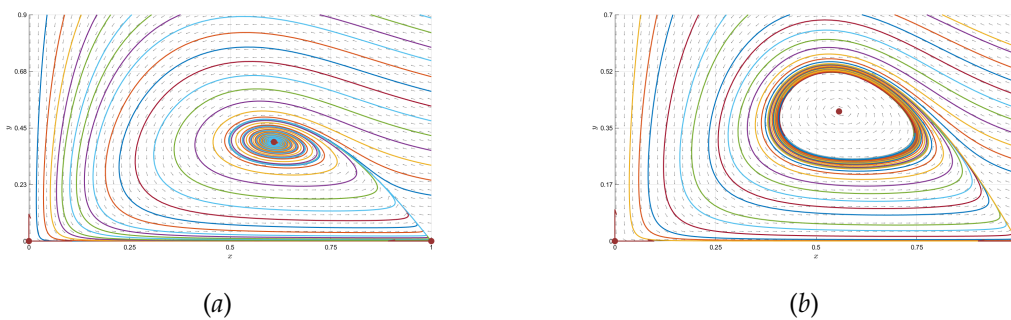
Figure 9: Phase portraits of the system (3) for $\mu = -0.3, \alpha = 0.5, \beta = 2, \delta = 0.94, e = 0.3$ and parameter h is varied; (a) Interior equilibria E_2 is stable for $h = 0.11$; (b) Existence of stable limit cycle enclosing an unstable hyperbolic focus, for $h = 0.08$. Stability of equilibrium points corresponding to these phase portraits is summarized in Table 4.

h	Equilibria	Eigenvalues		Stability	Remark
		$Re(\lambda_1)$	$Re(\lambda_2)$		
0.11	$E_0(0,0)$	-1.30667	0.3	saddle	E_2 globally
	$E_1(1,0)$	-1.3	0.02667	saddle	stable
	$E_2(0.60923, 0.39411)$	-0.01537	-0.01537	stable	
0.08	$E_0(0,0)$	-1.20667	0.3	saddle	Globally stable
	$E_1(1,0)$	-1.3	0.12667	saddle	limit cycle
	$E_2(0.55717, 0.40128)$	0.01723	0.01723	unstable	around E_2

Table 4: Summary of the stability of equilibrium points corresponding to the phase portraits presented in Figure 9.

Next, we focus on the two-parameter bifurcation diagrams of BT bifurcation for both strong and weak Allee effect, where the bifurcation parameters are β and h.

Example 6.3. *Let $\mu = 0.3, \alpha = 0.4, e = 0.3$. The system (3) has an unique equilibrium $E_4(0.805104, 0.118634)$ which is cusp of codimension 2 when $\beta = \beta_{BT} = 1.55062, \delta = \delta_* = 0.3867, h = h_{BT} = 0.271792$, because $W_4 = 2.28557 > 0$. Also $Z_4 = -0.0225877 \neq 0$. Therefore, the system (3) undergoes Bogdanov-Takens bifurcation around E_4 which includes supercritical Hopf bifurcation when (β, h) is varied near (β_{BT}, h_{BT}). The bifurcation diagram is given in Fig. 10-(a). $SN = SN^- \cup SN^+$ curve is red, H curve is blue, and HL curve is green and these three bifurcation curves partition the whole (β, h) parametric plane into four sub-regions, which are labelled as R_i, $i = 1, 2, 3, 4$. The region R_1 is above SN curve, the region R_2 is between SN^- and H curve, the region R_3 is between H and HL curve, and the region R_4 is below HL curve. Let us now describe how the dynamics of the system (3) change mainly for the interior equilibrium points as the parameters move through different sub-regions R_i, $i = 1, 2, 3, 4$. A description of the dynamics in these different regions is given below and summarized in Table 5.*

- *There is no interior equilibria when the parameters are in the region R_1 (Fig. 10-(b)).*

- *As parameters moves from R_1 to R_2, through saddle-node bifurcation, two interior equilibria appears: a stable focus or node E_2 and a saddle E_3 (Fig. 10-(c)).*

- *If parameters moves from R_2 to R_3, through supercritical Hopf bifurcation, the number of interior equilibrium points remains same but the stability of an interior equilibrium point E_2 is changed, while E_3 is still a saddle; E_2 becomes an unstable focus surrounded by a stable limit cycle (Fig. 10-(d)).*

- *If parameters lie on the curve HL, the stable homoclinic orbit occur for the system at the saddle E_3 and an unstable focus E_2 is inside homoclinic loop (Fig. 10-(e)).*

- *If parameters pass over HL curve and enter to the region R_4, homoclinic orbit is destroyed. Thus, in R_4, the system (3) only has two interior equilibria: the unstable focus E_2 and saddle E_3 (Fig. 10-(f)).*

- *Finally, as parameters moves from R_4 to R_1, through saddle-node bifurcation, two unstable interior equilibria disappears.*

(a) $\beta_{\mathrm{BT}} = 1.55062, h_{\mathrm{BT}} = 0.271792$

(b) $\beta = 1.1, h = 0.15$

(c) $\beta = 1.1, h = 0.144$

(d) $\beta = 1.1, h = 0.142$

(e) $\beta = 1.1, h = 0.140426$
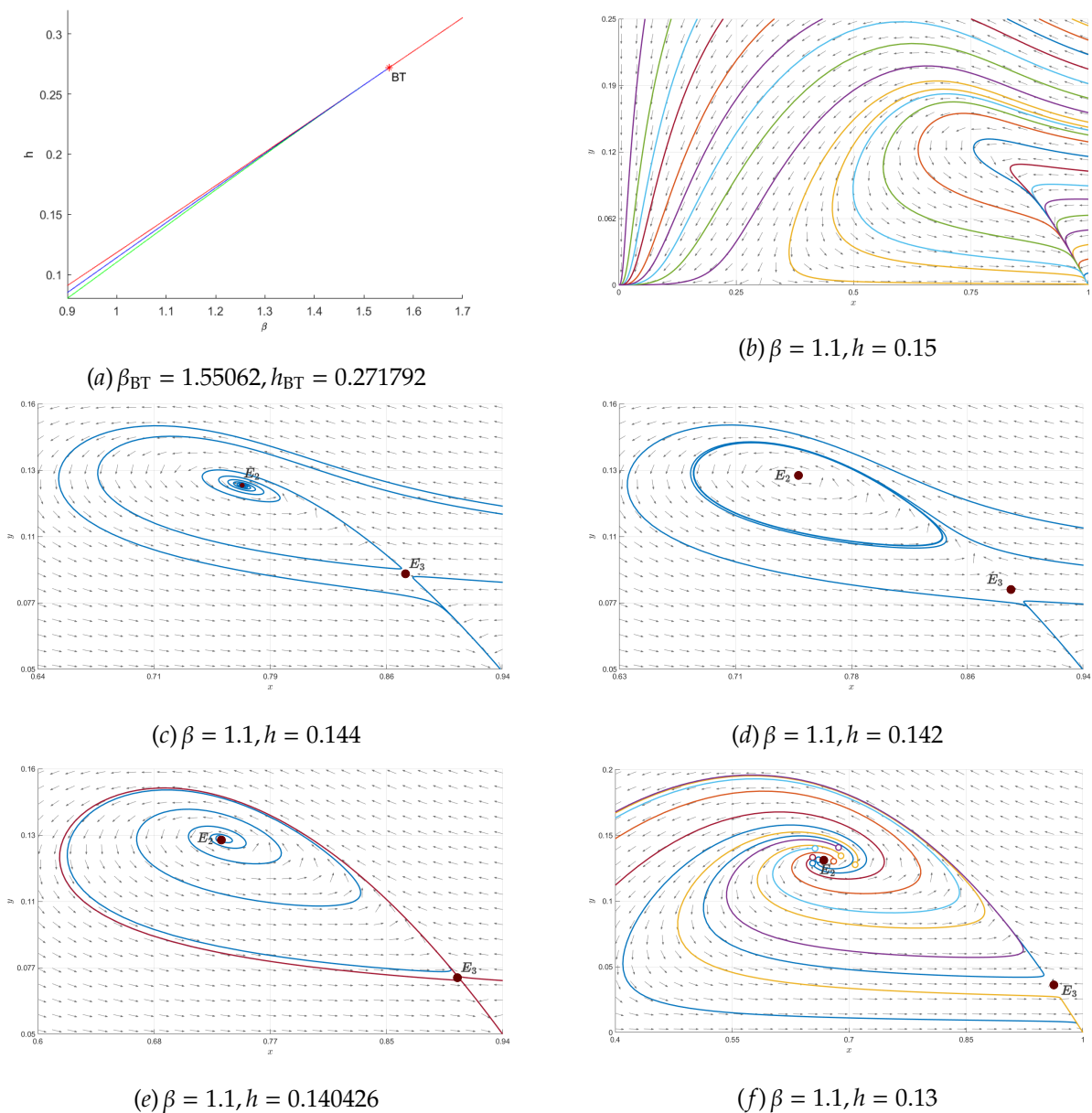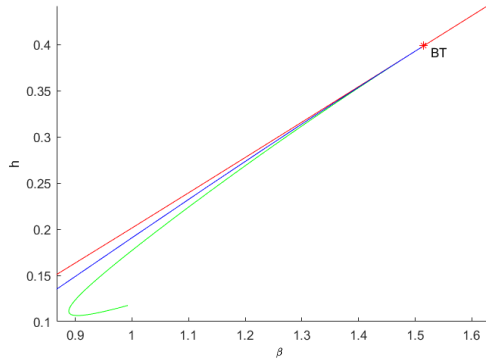
(f) $\beta = 1.1, h = 0.13$

Figure 10: Parameters: $\mu = 0.3, \alpha = 0.4, \delta = 0.3867, e = 0.3$; (a) Supercritical Bogdanov-Takens bifurcation diagram in (β, h)-plane. SN curve is red, H curve is blue, and HL curve is green; (b) − (f) Phase portraits of the system (3) when parameters β and h are varied; (b) $(\beta, h) \in R_1$: no interior equilibria; (c) $(\beta, h) \in R_2$: two interior equilibria exists ∼ a stable focus and a saddle; (d) $(\beta, h) \in R_3$: a stable limit cycle occurs surrounding an unstable focus and another equilibrium is a saddle; (e) $(\beta, h) \in$ HL: a stable homoclinic orbit at the saddle occurs and inside hoomoclinic loop second equilibrium is an unstable focus; (f) $(\beta, h) \in R_4$: two interior equilibria exists ∼ an unstable focus and a saddle.

| Region	(β, h)	No. of equilibria	Equilibria	Eigenvalues		Stability	Remark
				$\mathrm{Re}(\lambda_1)$	$\mathrm{Re}(\lambda_2)$		
R_1	$(1.1, 0.15)$	3	$E_0(0,0)$	-0.8867	-0.3	stable	
			$E_1(1,0)$	-0.7	-0.100986	stable	bi-stable
			$E_\mu(0.3,0)$	-0.415271	0.21	saddle	
R_2	$(1.1, 0.144)$	5	$E_0(0,0)$	-0.8667	-0.3	stable	
			$E_1(1,0)$	-0.7	-0.08099	stable	
			$E_\mu(0.3,0)$	-0.39527	0.21	saddle	tri-stable
			$E_2(0.77231, 0.12607)$	-0.00903	-0.00903	stable	
			$E_3(0.87751, 0.09037)$	-0.30816	0.04287	saddle	
R_3	$(1.1, 0.142)$	5	$E_0(0,0)$	-0.86003	-0.3	stable	tri-stable
			$E_1(1,0)$	-0.7	-0.07432	stable	Stable limit
			$E_\mu(0.3,0)$	-0.38861	0.21	saddle	cycle around
			$E_2(0.75009, 0.12936)$	0.01143	0.01143	unstable	E_2
			$E_3(0.89742, 0.07951)$	-0.36959	0.0463	saddle	
HL	$(1.1, 0.140426)$	5	$E_0(0,0)$	-0.85479	-0.3	stable	tri-stable
			$E_1(1,0)$	-0.7	-0.06907	stable	The homoclinic
			$E_\mu(0.3,0)$	-0.38336	0.21	saddle	loop at the
			$E_2(0.73608, 0.13075)$	0.0234	0.0234	unstable	saddle E_3
			$E_3(0.90961, 0.07217)$	-0.40723	0.0464	saddle	around E_2
R_4	$\$(1.1, 0.13)$	5	$E_0(0,0)$	-0.82003	-0.3	stable	bi-stable
			$E_1(1,0)$	-0.7	-0.03432	stable	Limit cycle
			$E_\mu(0.3,0)$	-0.34861	0.21	saddle	disappears
			$E_2(0.66952, 0.13061)$	0.07094	0.07094	unstable	through homo-clinic
			$E_3(0.96382, 0.03276)$	-0.57909	0.02959	saddle	bifurcation

Table 5: Summary of the number and stability of equilibrium points corresponding to the different domains of the bifurcation diagram presented in Figure 10.

Example 6.4. *Let $\mu = -0.3, \alpha = 0.5, e = 0.3$. The system (3) has an unique equilibrium $E_4(0.70609, 0.356641)$ which is cusp of codimension two when $\beta = \beta_{BT} = 1.51512, \delta = \delta_* = 0.27988, h = h_{BT} = 0.398666$, because $W_4 = 2.39474 > 0$. Also $Z_4 = -0.137163 \neq 0$. Therefore, the system (3) undergoes Bogdanov-Takens bifurcation around E_4 which includes supercritical Hopf bifurcation when (β, h) is varied near (β_{BT}, h_{BT}). The bifurcation diagram is given in Fig. 11-(a). As in the previous example, SN curve is red, H curve is blue, and HL curve is green and these three bifurcation curves partition the whole (β, h) parametric plane into four sub-regions R_i, $i = 1, 2, 3, 4$. A description of the dynamics in these different regions is given below and summarized in Table 6.*

- *There is no interior equilibria when the parameters are in the region R_1 (Fig. 11-(b)).*

- *As parameters moves from R_1 to R_2, through saddle-node bifurcation, two interior equilibria appears: a stable focus or node E_2 and a saddle E_3 (Fig. 11-(c)).*

- *If parameters moves from R_2 to R_3, through supercritical Hopf bifurcation, the number of interior equilibrium points remains same but the stability of an interior equilibrium point E_2 is changed, while E_3 is still a saddle; E_2 becomes an unstable focus surrounded by a stable limit cycle (Fig. 11-(d)).*

- *If parameters lie on the curve HL, the stable homoclinic orbit occur for the system at the saddle E_3 and an unstable focus E_2 is inside homoclinic loop (Fig. 11-(e)).*

- *If parameters pass over HL curve and enter to the region R_4, homoclinic orbit is destroyed. Thus, in R_4, the system (3) only has two interior equilibria: the unstable focus E_2 and saddle E_3 (Fig. 11-(f)).*

- *Finally, as parameters moves from R_4 to R_1, through saddle-node bifurcation, two unstable interior equilibria disappears.*
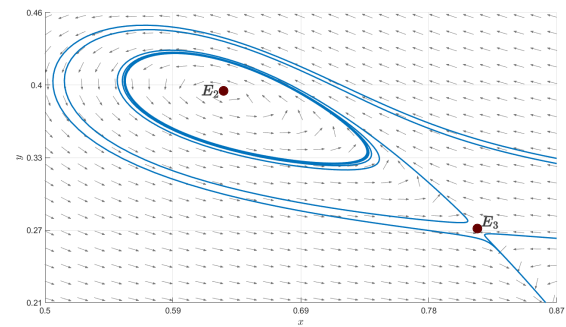
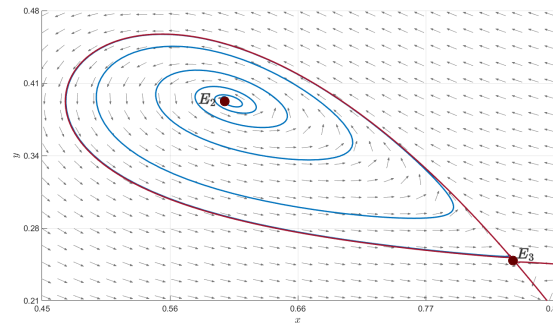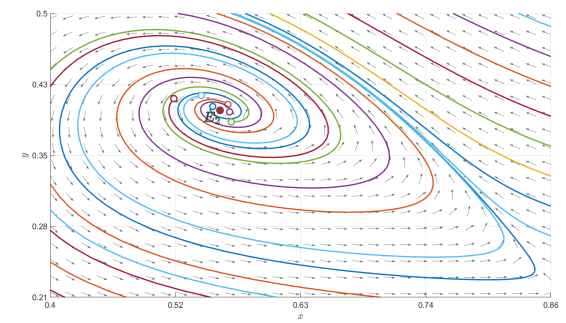(a) $\beta_{BT} = 1.51512, h_{BT} = 0.398666$
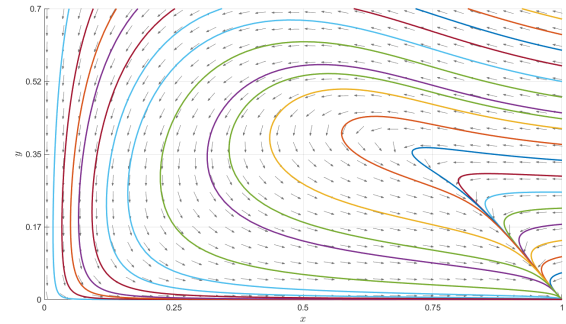
(b) $\beta = 1.1, h = 0.25$
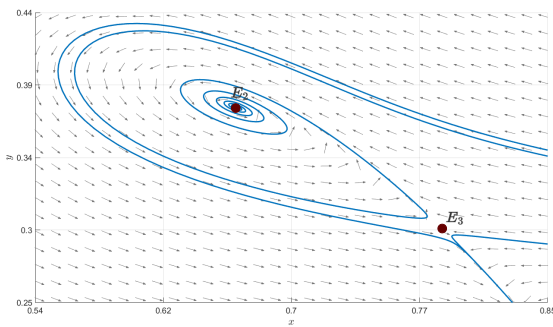
(c) $\beta = 1.1, h = 0.235$

(d) $\beta = 1.1, h = 0.23$

(e) $\beta = 1.1, h = 0.22410665$

(f) $\beta = 1.1, h = 0.21$

Figure 11: Parameters: $\mu = -0.3, \alpha = 0.5, \delta = 0.27988, e = 0.3$; (a) Supercritical Bogdanov-Takens bifurcation diagram in (β, h)-plane. SN curve is red, H curve is blue, and HL curve is green; (b) − (f) Phase portraits of the system (3) when parameters β and h are varied; (b) $(\beta, h) \in R_1$: no interior equilibria; (c) $(\beta, h) \in R_2$: two interior equilibria exists ∼ a stable focus and a saddle; (d) $(\beta, h) \in R_3$: a stable limit cycle occurs surrounding an unstable focus and another equilibrium is a saddle; (e) $(\beta, h) \in$ HL: a stable homoclinic orbit at the saddle occurs and inside homoclinic loop second equilibrium is an unstable focus; (f) $(\beta, h) \in R_4$: two interior equilibria exists ∼ an unstable focus and a saddle.

Region	(β, h)	No. of equilibria	Equilibria	Eigenvalues		Stability	Remark
				$\mathrm{Re}(\lambda_1)$	$\mathrm{Re}(\lambda_2)$		
R_1	$(1.1, 0.25)$	2	$E_0(0,0)$	-1.11321	0.3	saddle	E_1 globally
			$E_1(1,0)$	-1.3	-0.37988	stable	stable
R_2	$(1.1, 0.235)$	4	$E_0(0,0)$	-1.06321	0.3	saddle	bi-stable
			$E_1(1,0)$	-1.3	-0.32988	stable	
			$E_2(0.66149, 0.37804)$	-0.01674	-0.01674	stable	
			$E_3(0.78613, 0.29876)$	-0.44966	0.10177	saddle	
R_3	$(1.1, 0.23)$	4	$E_0(0,0)$	-1.04655	0.3	saddle	bi-stable
			$E_1(1,0)$	-1.3	-0.31321	stable	Stable cycle
			$E_2(0.63175, 0.38832)$	0.01203	0.01203	unstable	around E_2
			$E_3(0.81308, 0.2732)$	-0.55155	0.1186	saddle	
HL	$(1.1, 0.224107)$	4	$E_0(0,0)$	-1.0269	0.3	saddle	bi-stable; The
			$E_1(1,0)$	-1.3	-0.29357	stable	homoclinic loop
			$E_2(0.6052, 0.39497)$	0.03504	0.03504	unstable	at the saddle
			$E_3(0.83631, 0.24856)$	-0.63886	0.12697	saddle	E_3 around E_2
R_4	$\$(1.1, 0.21)$	4	$E_0(0,0)$	-0.97988	0.3	saddle	E_1 globally
			$E_1(1,0)$	-1.3	-0.24655	stable	stable. Limit
			$E_2(0.5563, 0.40133)$	0.07096	0.07096	unstable	cycle disappears through
			$E_3(0.87719, 0.1991)$	-0.7946	0.12964	saddle	homoclinic bifurcation

Table 6: Summary of the number and stability of equilibrium points corresponding to the different domains of the bifurcation diagram presented in Figure 11.

7. Basins of attraction

A bifurcation analysis shows that our ecological model (3) generates multiple attractors. The basin of attraction $\mathcal{B}(x^\star)$ of the stable equilibria $x^\star$ is the set of all points in phase space that converge to $x^\star$ in forward time. The basin of attraction $\mathcal{B}(\gamma)$ of the stable limit cycle (separatrix cycle) γ is the set of all points in phase space that converge to this limit cycle (separatrix cycle) in forward time. In this section we discuss the basins of attraction of all possible attractors, as we will determine separatrices in the phase plane separating basins of attraction related to co-existence, extinction of both predator and prey population and extinction of predator population. Since stable and unstable manifolds of saddle points E_1, E_3 and E_μ acts as separatrix curve between basins of attraction of multiple attractors, let $W^u_\nwarrow(E_3)$ be the branch of the unstable manifold of the saddle E_3 that goes up to the left, $W^s_\nwarrow(E_3)$ and $W^s_\searrow(E_3)$ be the branches of the stable manifold of the saddle E_3 that goes up to the left and down to the right, $W^s_\swarrow(E_\mu)$ be the branch of the stable manifold of the saddle E_μ that goes down to the left and $W^u_\nwarrow(E_1)$ be the branch of the unstable manifold of the saddle E_1 that goes up to the left.

Strong Allee effect (SAE): In the case of strong Allee effect the origin is always an attractor. Moreover, system may have three more attractors, either a locally asymptotically stable equilibria or a stable limit cycle or a stable separatrix cycle.

(i) If $\beta \le \delta$, it follows that $H_2 < 0$, so that $h > H_2$, implies that E_1 is locally asymptotically stable. Stable manifold $W^s_\swarrow(E_\mu)$ of the saddle E_μ acts as separatrix curve between basins of attraction $\mathcal{B}(E_0)$ (yellow) and $\mathcal{B}(E_1)$ (green), shown in Figure 12. Solutions with initial values in yellow colored area converge towards the origin, leading to the extinction of both species. Solutions with initial values in green colored area converge towards the locally asymptotically stable predator-free equilibrium E_1, corresponding to the extinction of predators.

(ii) If $\beta > \delta$, $H_1 > 0$ and $h \le H_1$ by Theorem 4.1, a trivial equilibrium is globally asymptotically stable.

(iii) If $\beta > \delta$, $H_2 > 0$ and $H_1 < h < H_2$, there are two types of bistability: bistability between the origin
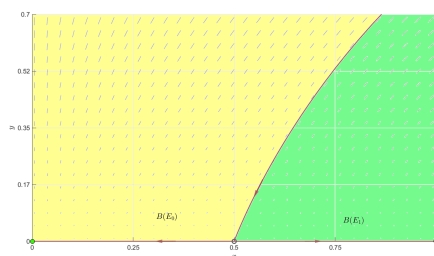
Figure 12: Basins of attraction $\mathcal{B}(E_0)$ (yellow) and $\mathcal{B}(E_1)$ (green) in the system (3) for $0 < \mu < 1, \beta \leq \delta$.

and a stable coexistence equilibrium E_2, and between the origin and a stable limit cycle Γ. In both cases, stable manifold $W^s_{\nearrow}(E_\mu)$ acts as separatrix curve between two basins of attraction (Fig. 13-(a,b)). Solutions with initial values in yellow colored area will be driven to the extinction of both species, while solutions with initial values in blue colored area will tend either to the locally asymptotic stable focus, corresponding to the stable periodic coexistence, or to the stable limit cycle, that is the prey and predator will oscillate periodically. In the case in which a limit cycle disappears, since the unstable manifold $W^u_{\nwarrow}(E_1)$ is above the stable manifold $W^s_{\nearrow}(E_\mu)$, for all initial values which don't belong to the stable manifold of E_μ, trajectories will be attracted to E_0 (Fig. 13-(c)).

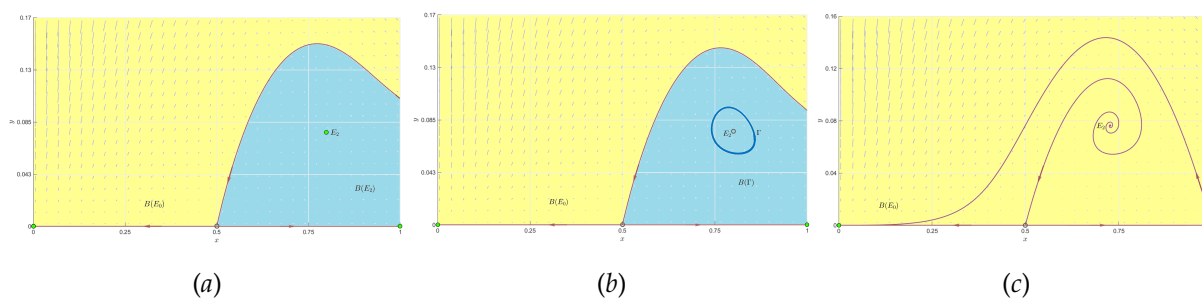| (a) | (b) | (c) |

Figure 13: Basins of attraction in the system (3) for $0 < \mu < 1, \beta > \delta$ and $H_1 < h \leq H_2, H_2 > 0$: $\mathcal{B}(E_0)$ (yellow region); (a) $\mathcal{B}(E_2)$ (blue region); (b) $\mathcal{B}(\Gamma)$ (blue region); (c) E_2 is unstable and the stable limit cycle disappears.

(iv) If $\beta > \delta$ and $h > H_2$, the equilibrium E_1 is locally asymptotically stable. The interior equilibrium E_2, if exists, may change its stability through supercritical Hopf bifurcation. In Section 6 through numerical simulation the emergence of homoclinic loop has been shown, when the limit cycle collides with a saddle point. The model produces a homoclinic bifurcation curve, and for parameter values on HL curve, the homoclinic loop Γ_0 at the saddle E_3 appears around an unstable equilibrium, creating the stable separatrix cycle $\Gamma = \Gamma_0 \cup \{E_3\}$. This results in either a bi-stability or a tri-stable phenomenon. There are three types of tri-stability: between the origin, predator-free equilibrium and a stable coexistence equilibrium E_2, between the origin, predator-free equilibrium and a limit cycle Γ and between the origin, predator-free equilibrium and the stable separatrix cycle Γ. In the case in which a limit cycle disappears and in which there is no interior equilibria, system demonstrates the bi-stability between the origin and predator-free equilibrium. So, we have five distinct multi-stability regimes, in which we will consider the respective basins of attractions:

(iv-1) if interior equilibrium E_2 is a locally asymptotic stable, the system has three attractors: the origin, predator-free equilibrium and a stable coexistence equilibrium. Their basins of attraction $\mathcal{B}(E_0)$ (yellow), $\mathcal{B}(E_1)$ (green) and $\mathcal{B}(E_2)$ (blue) are shown in Figure 14-(a). The stable manifold $W^s_{\nearrow}(E_\mu)$ of the saddle E_μ acts as separatrix curve between basins of attraction $\mathcal{B}(E_0)$ and $\mathcal{B}(E_1)$, while both stable manifolds $W^s_{\nwarrow}(E_3)$ and $W^s_{\searrow}(E_3)$ of the saddle E_3 acts as separatrix curves between
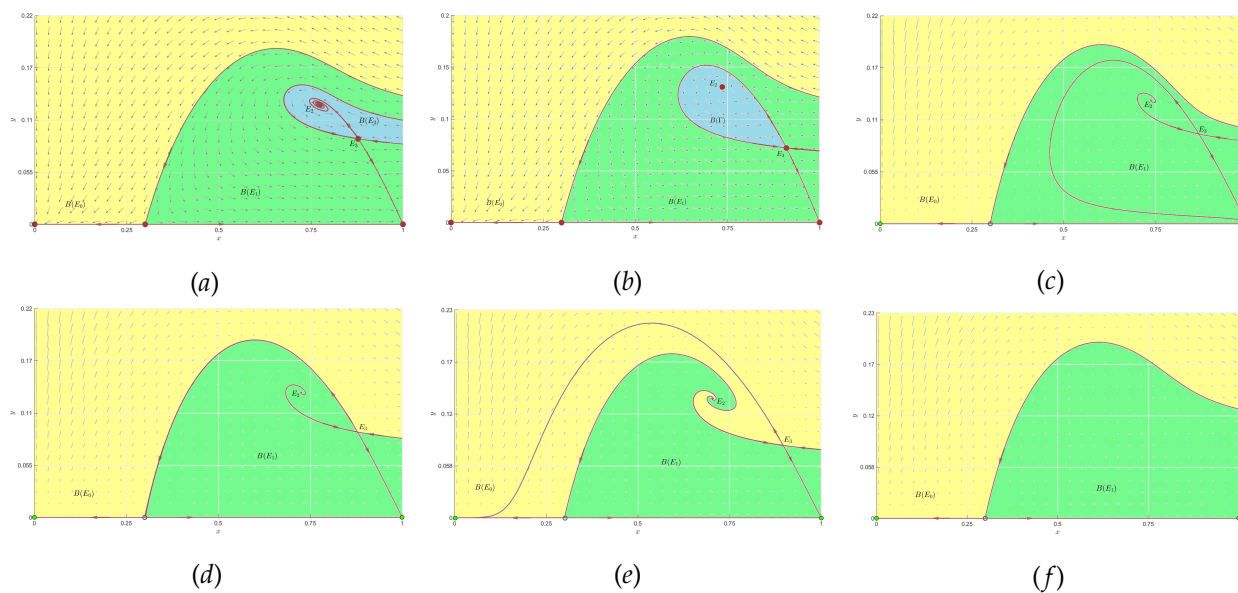
Figure 14: Basins of attraction in the system (3) for $\mu > 0, \beta > \delta$ and $h > H_2$. $\mathcal{B}(E_0)$ (yellow), $\mathcal{B}(E_1)$ (green), $\mathcal{B}(E_2)$ and $\mathcal{B}(\Gamma)$ (blue); (*a*) E_2 is asymptotically stable; (*b*) E_2 is unstable and a stable separatrix cycle Γ exists; (*c*) E_2 is unstable and $W^u_{\nwarrow}(E_3)$ is below $W^s_{\swarrow}(E_\mu)$; (*d*) E_2 is unstable and heteroclinic connection from E_3 to E_μ exists; (*e*) E_2 is unstable and $W^u_{\nwarrow}(E_3)$ is above $W^s_{\swarrow}(E_\mu)$; (*f*) No interior equilibria.

basins of attraction $\mathcal{B}(E_1)$ and $\mathcal{B}(E_2)$. Solutions with initial values in yellow colored area will be driven to the extinction of both species, solutions with initial values in green colored area converge towards the locally asymptotically stable predator-free equilibrium E_1, corresponding to the extinction of predators and solutions with initial values in blue colored area will tend to the locally asymptotic equilibrium, corresponding to the stable periodic coexistence.

(iv-2) if E_2 is an unstable focus surrounded by a stable limit cycle Γ, the system has three attractors: the origin, predator-free equilibrium and a stable limit cycle γ. Separatrix curves for the respective basins of attraction $\mathcal{B}(E_0)$, $\mathcal{B}(E_1)$ and $\mathcal{B}(\gamma)$ are the same as in the previous case (iv-2).

(iv-3) if E_2 is a locally unstable focus surrounded by a stable separatrix cycle Γ, the system has three attractors: the origin, predator-free equilibrium and a stable separatrix cycle Γ. Their basins of attraction $\mathcal{B}(E_0)$ (yellow), $\mathcal{B}(E_1)$ (green) and $\mathcal{B}(\Gamma)$ (blue) are shown in Figure 14-(b). In this case, solutions with initial values inside the separatrix cycle Γ converge towards this cycle, while solutions with initial values outside the separatrix cycle Γ converge either towards the origin or to predator-free equilibrium. The stable manifold $W^s_{\swarrow}(E_\mu)$ acts as separatrix curve between two basins of attraction $\mathcal{B}(E_0)$ and $\mathcal{B}(E_1)$.

(iv-4) if E_2 is a locally asymptotically unstable and there is no closed orbits, the system has two attractors: the origin and the predator-free equilibrium. In order to discuss basins of attraction in this case, we first prove the existence of a heteroclinic connection between two saddles E_3 and E_μ, which is a subset of $W^u_{\nwarrow}(E_3) \cap W^s_{\swarrow}(E_\mu)$.

Theorem 7.1. *Let $\mu > 0, \beta > \delta, h > H_2$. If E_2 is an asymptotically unstable equilibrium and there are no closed orbits in the system* (3), *there exist values of parameters for which the unstable manifold of the saddle E_3 and the stable manifold of the saddle E_μ form the heteroclinic orbit from E_3 to E_μ.*

Proof. In this case, E_0 and E_1 are attractors. The ω-limit of the trajectory determined by $W^u_{\nwarrow}(E_3)$ remains at Ω since it's an invariant region. If the α-limit of the trajectory starting from any point from $W^s_{\swarrow}(E_\mu)$ is outside of Ω, then the trajectory determined by $W^u_{\nwarrow}(E_3)$ is below the trajectory

determined by $W^s_\swarrow(E_\mu)$ (Fig. 14-(c)). If the α-limit of the trajectory starting from any point from $W^s_\swarrow(E_\mu)$ is in Ω, it must be the unstable focus E_2 and the trajectory determined by $W^u_\nwarrow(E_3)$ is above the trajectory determined by $W^s_\swarrow(E_\mu)$ (Fig. 14-(e)). Therefore, since these two trajectories determined by $W^u_\nwarrow(E_3)$ and by $W^s_\swarrow(E_\mu)$ can not intersect, because of the theorem of existence and uniqueness of solutions [8], there exist value of parameter h for which those two trajectories coincide, forming the heteroclinic connection between E_3 and E_μ (Fig. 14-(d)). □

Therefore, to determine separatrices between $\mathcal{B}(E_0)$ and $\mathcal{B}(E_1)$, we distinguish three subcases:

(iv-4(a)) if $W^u_\nwarrow(E_3)$ is below $W^s_\swarrow(E_\mu)$, $W^s_\swarrow(E_\mu)$ acts as separatrix curve between two basins of attraction $\mathcal{B}(E_0)$ and $\mathcal{B}(E_1)$ (Figure 14-(c)).

(iv-4(b)) if there exists the heteroclinic connection from E_3 to E_μ which is a subset of $W^u_\nwarrow(E_3) \cap W^s_\swarrow(E_\mu)$, this heteroclinic orbit together with $W^s_\nwarrow(E_3)$ serve as separatrix curves between two basins of attraction $\mathcal{B}(E_0)$ and $\mathcal{B}(E_1)$ (Figure 14-(d)).

(iv-4(c)) if $W^u_\nwarrow(E_3)$ is above $W^s_\swarrow(E_\mu)$, then both trajectories determined by $W^s_\searrow(E_3)$ and $W^s_\swarrow(E_\mu)$ approach the unstable focus as $t \to -\infty$. The basins of attraction are divided by these two trajectories and a stable manifold $W^s_\nwarrow(E_3)$ of E_3 (Figure 14-(e)).

(iv-5) if there is no interior equilibria, system demonstrates the bi-stability between the origin and predator-free equilibrium and the stable manifold $W^s_\swarrow(E_\mu)$ acts as separatrix curve between basins of attraction $\mathcal{B}(E_0)$ (yellow) and $\mathcal{B}(E_1)$ (green), shown on Figure 14-(f). Solutions with initial values in yellow colored area will be driven to the extinction of both species and solutions with initial values in green colored area converge towards the locally asymptotically stable predator-free equilibrium E_1, corresponding to the extinction of predators.

Weak Allee effect (WAE): In the case of weak Allee effect, the origin is an unstable node.

(i) If $\beta > \delta$, $H_2 > 0$ and $h < H_2$, the predator-free equilibrium E_1 is unstable and the interior equilibrium E_2 may change its stability through supercritical Hopf bifurcation. Thus, for any value of parameters, there exists an attractor in the first quadrant - the stable coexistence equilibrium E_2 or the stable limit cycle Γ, so that depending on values of parameters, populations will persist with either stable periodic or oscillatory periodic behavior. Therefore, in the case of weak Allee effect, the model is not necessarily a bistable system.

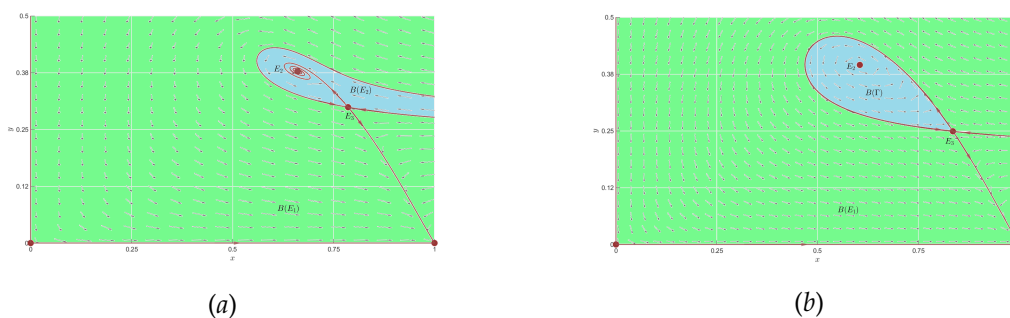|	
(a)	(b)

Figure 15: Basins of attraction in the system (3) for $\mu < 0, \beta > \delta, h > H_2$. $\mathcal{B}(E_1)$ (green) and $\mathcal{B}(E_2)$ and $\mathcal{B}(\Gamma)$ (blue) ; (a) E_2 is asymptotically stable; (b) E_2 is unstable and stable separatrix cycle Γ exists.

(ii) If $\beta > \delta$ and $h > H_2$, predator-free equilibrium E_1 is asymptotically stable and the interior equilibrium E_2, if exists, may change its stability through supercritical Hopf bifurcation. System (3) demonstrates three types of bistability: bistability between the predator-free equilibrium and a stable coexistence equilibrium E_2, between the predator-free equilibrium and a stable limit cycle γ and between the predator-free equilibrium and a stable separatrix cycle Γ. We have three distinct bistability regimes, in which we will consider the respective basins of attractions:

(ii-1) If E_2 is asymptotically stable, the basins of attraction $\mathcal{B}(E_1)$ (green) and $\mathcal{B}(E_2)$ (blue) are divided by the stable manifolds $W^s_{\nearrow}(E_\mu)$ of saddle E_3 (Fig. 15-(a)).

(ii-2) If E_2 is unstable surrounded by stable limit cycle γ, the basins of attraction $\mathcal{B}(E_1)$ and $\mathcal{B}(\gamma)$ is the same as in the previous case (ii-1).

(ii-3) If E_2 is unstable surrounded by stable separatrix cycle Γ, basins of attraction $\mathcal{B}(E_0)$ (green) and $\mathcal{B}(\Gamma)$ (blue) are shown in Figure 15-(b). In this case, solutions with initial values inside the separatrix cycle Γ converge towards this cycle, while solutions with initial values outside the separatrix cycle Γ converge towards the predator-free equilibrium.

8. Concluding remarks with ecological implications

In this paper, we studied the predator-prey model with Holling type II functional response, Allee effect in prey, and predator nonlinear harvesting. Our model can be applied to the prey and predator relationship between cod (Gadus Morhua) and sharks. In this scenario, cod are exposed to the Allee effect (also called depensation by fisheries biologists - see [32, 36]) due to their difficulties in finding mates at low population densities, while sharks are hunted by humans for their fins [2, 14, 16]. The application of our model extends to other predator-prey interactions where the prey is influenced by the Allee effect and the predator is harvested for commercial purposes. Examples of such interactions include Atlantic cod-herring ([37, 38]), Pacific salmon-anchovies ([15, 40]), sea lions-Pacific salmon ([20, 36]), etc.

Firstly, the original system is simplified to a topologically equivalent predator-prey system (3) with six parameters using an appropriate scaling. It is shown that the system (3) has important biological properties such as positivity, uniform boundedness, and sufficient conditions for uniform permanence of the system in the case of weak Allee effect has been obtained.

The local and global stability of different equilibria of the system has been discussed. It was shown that the origin is a saddle in the case of weak Allee effect (WAE) and locally asymptotic stable equilibrium in the case of strong Allee effect (SAE). In the case of SAE, conditions for the global stability of the origin are obtained. In both WAE and SAE cases, the system has the predator-free equilibrium $E_1(1, 0)$ which is a stable hyperbolic node for $h > H_2$, and a hyperbolic saddle for $h < H_2$. In the case of WAE, conditions for global stability of the predator-free equilibrium are obtained. The additional predator-free equilibrium $E_\mu(\mu, 0)$ exists in the case of SAE. This equilibrium is an unstable hyperbolic node for $h < H_1$, and a hyperbolic saddle for $h > H_1$. For both WAE and SAE scenarios, the proposed system doesn't have interior equilibria or have one or two positive interior equilibrium points for different values of parameters. It is found that if two interior equilibrium points exist, one of them is always a saddle point and the other changes its stability.

Next, bifurcations of the system have been studied. It is observed that the proposed system exhibits very complex dynamics and many local and global bifurcations like transcritical, pitchfork, saddle-node, Hopf, homoclinic and Bogdanov-Takens (BT) have been identified. In order to examine the effect of nonlinear harvesting on the dynamics of the system we choose h as the bifurcation parameter. Two transcritical bifurcations give a rise of interior equilibria: E_2 through E_μ at the bifurcation threshold $h = H_1 > 0$ and E_3 through E_1 at the bifurcation threshold $h = H_2 > 0$. The first transcritical bifurcation only appears in the case of SAE. In the special case if $\beta = \widehat{\beta_2}$, where $\widehat{\beta_2}$ is given by (10), the system undergoes a pitchfork bifurcation at the bifurcation threshold $h = H_2 > 0$, which includes the disappearance of the stable equilibrium E_2 through E_1 by increasing h. First transcritical bifurcation occurs only in the case of SAE and it does not significantly change the dynamics of the system. However, the second transcritical bifurcation at the bifurcation threshold $h = H_2 > 0$ transforms a predator extinction equilibrium point E_1 into a stable equilibrium point by increasing the maximal harvesting rate of the predator species h above this threshold, while the interior equilibrium that appears through this bifurcation is unstable. Pitchfork bifurcation at the bifurcation threshold $h = H_2 > 0$ has a similar influence on the dynamics of the system. It is observed that through this bifurcation a predator extinction equilibrium point E_1 changes its stability into a stable equilibrium while the stable coexistence equilibrium disappears by increasing the bifurcation parameter h above the critical value $h = H_2 > 0$. Therefore, in the case of WAE, these two local bifurcations

at the predator-free equilibrium E_1 provide the limit for continuous harvesting without putting the predator species at risk of extinction.

Next, conditions under which the interior equilibrium changes its stability through Hopf bifurcation have been given, and the appearance of a stable limit cycle around coexistence equilibrium through the supercritical Hopf bifurcation has been shown numerically, in both cases of WAE and SAE. From an ecological point of view, Hopf bifurcation indicates coexistence of predator and prey, with either stable oscillations of both populations or a stable periodic coexistence. The emergence of a homoclinic loop has been shown through numerical simulation when the limit cycle arising through Hopf bifurcation collides with a saddle point. It is shown that a system can experience the Bogdanov-Takens bifurcation at the interior equilibrium which is the cusp of codimension 2. The non-degeneracy conditions of the Bogdanov-Takens bifurcation were also proved. In both WAE and SAE cases, we provided the bifurcation diagrams in (β, h)-plane for the Bogdanov-Takens bifurcation which includes saddle-node bifurcation, supercritical Hopf bifurcation and homoclinic bifurcation (Figs. 10a and 11a). We give concluding remarks with a biological implication for these bifurcation diagrams. In both the strong and weak Allee effect the Bogdanov-Takens bifurcation demonstrates that there exists a great possibility of extinction of predator and prey population, when parameters belong to the region R_1 (in which there are no interior equilibria) and R_4 (in which there is no interior attractor). But, there is a difference between SAE and WAE. While in the case of SAE, depending on the initial conditions, it is possible the extinction of both populations or just the predator population, in the case of WAE, only the extinction of the predator population is possible. However, there are two small parametric regions R_2 and R_3 in which either the predator and prey coexist or the predator or both species can be driven to extinction, depending upon the initial values. The model produces a homoclinic curve HL in the bifurcation plane which gives the limit for the existence of the closed orbit and periodic coexistence of species. Also, the model has produced a saddle-node bifurcation curve which confirms the appearance or disappearance of interior fixed points. The significant change in the behavior of the model due to saddle-node bifurcations is evident in the transition from the region R_1 to R_2 and from the region R_4 to R_1. However, the existence of BT point produces two qualitatively different saddle-node bifurcations: first, from the region R_2 to the region R_1 when the stable periodic coexistence is destroyed and all solution trajectories settle to the predator population extinction or even to total extinction in the case of SAE and the second from the region R_4 to R_1, when two unstable coexistence equilibrium points are destroyed, so that such saddle-node bifurcation does not affect the existence of the internal attractor. Thus, the saddle-node and homoclinic bifurcations lead to potentially dramatic shifts in the system dynamics.

Bifurcation analysis shows that the proposed model generates multiple attractors in a small parametric region. The existence of separatrix curves (stable and unstable manifold of saddles) which separate the behavior of trajectories of the system is obtained, implying that the dynamic of the system is very sensitive to the initial conditions. In particular, in the case of SAE the existence of a heteroclinic connection between E_μ and the interior saddle point is proved, separating the basin of attractions of the origin and predator-free equilibrium E_1. In the case of SAE, a model may exhibit bi-stability either between the origin and a stable interior equilibrium point, between the origin and a stable predator-free equilibrium, between the origin and a stable limit cycle, or between the origin and a stable separatrix cycle. As a result, both populations may become extinct, the predator population may go extinct, or they may coexist. Furthermore, in the case of SAE, the proposed model may even exhibit tri-stability if both the coexistence equilibrium and predator-free equilibrium are asymptotically stable. In the case of WAE, a model may also exhibit bi-stability either between the predator-free equilibrium and stable interior equilibrium points, between the predator-free equilibrium and a stable limit cycle, or between the predator-free equilibrium and a stable separatrix cycle.

9. Conclusions

Taking into account the complete dynamics of the underlying system, we can conclude that the nonlinear Michaelis-Menten type predator harvesting has a different impact on the model (3) in the cases of strong and weak Allee effects on the prey population.

Extinction of both species is possible only in the case of SAE. If $\beta > \delta$, $H_1 > 0$, $h \le H_1$, the trivial equilibrium point is globally asymptotically stable. If the maximal harvesting rate of the predator species h

is below threshold $H_1 > 0$, the predator population size will be increased sufficiently to cause the extinction of the prey population and, consequently, the extinction of the predator population.

In the case of $\beta > \delta, H_2 > 0, H_1 < h \leq H_2$, the supercritical Hopf bifurcation leads to the possible coexistence of populations in both SAE and WAE. In the case of WAE, the system (3) has been proven to be uniformly permanent (Theorem 3.9), guaranteeing the long time survival of the species. Thus, the maximum threshold for continuous harvesting without the risk of the predator population extinction is obtained. On the other hand, in the case of SAE, the optimal harvesting rate of the predator population can only promote the coexistence of the population when the Allee effect is quite low. Otherwise, the predator harvesting ceases to have any stabilizing effect. By decreasing h enough, the limit cycle will disappear and, for all initial values which don't belong to the stable manifold of E_μ, trajectories will be attracted to the origin. Therefore, even if the maximal harvesting rate is slightly above the threshold $h = H_1$ total extinction is still possible.

If $\beta > \delta$ and $h > H_2$, in the case of WAE, the predator-free equilibrium is globally asymptotically stable if there are no interior equilibria. However, if the interior equilibria are unstable and there is no closed orbits, the predator will ultimately go extinct. In the case of SAE, the populations can also coexist, but with small varying of initial conditions, the orbits will be attracted to the predator-free equilibrium resulting only in the extinction of the predator population. If the interior equilibria don't exist or they are unstable and there is no closed orbits, a system experiences bistability between the origin and predator-free equilibrium. In both cases, it is observed that the probability of predator extinction increases at a higher rate of harvesting, while then their survival highly depends on the average time spent on processing food and the rate of conversion of consumed prey to predator.

If $\beta \leq \delta$, in the case of WAE, Theorem 4.3 ensures the extinction of the predator population. The extinction is caused by the higher mortality rate of predator since the condition $\beta < \delta$ is equivalent to $d > \theta K/b$. In the case of SAE the system experiences bistability between the origin and the predator-free equilibrium E_1 and trajectories of the model can have different behavior strongly depending on the initial conditions. The extinction of the predator is caused either by the extinction of the prey population or by the higher mortality rate of the predator.

For Gause type predator-prey model (1) without the influence of predator harvesting, it has been proven that the equilibrium at the origin of the model is an attractor for any set of parameters. When a unique positive equilibrium exists, it is possible for it to be an attractor or a repeller surrounded by a unique limit cycle. This results in a coexistence of predator and prey for certain initial conditions, with either stable oscillations of both populations or with a stable periodic coexistence. There are also initial values for which both species will go extinct. In order to study the conditions under which the extinction of both populations occurs, separatrix curves of the basins of attraction of multiple attractors were considered. The existence of a heteroclinic curve is proved. When this curve is broken by changing parameter values, the origin turns out to be an attractor for all orbits in the phase plane. Through a comparison of the dynamics of systems (1) and (2), we observed that nonlinear harvesting has a significant impact on the dynamics of system (1). It influences the number of equilibria and the bifurcation structure is richer than when the harvesting is absent. A system (3) may have two interior equilibria and allows the occurrence of Bogdanov-Takens bifurcation. In contrast to the results in the paper [21], we provided a detailed analysis of the proposed model with a weak Allee effect. In the case of SAE, bistability between the origin and predator-free equilibria, and between the origin and interior attractor (equilibrium or limit cycle) has been observed in both models. The main difference is tristability between the origin, predator-free equilibria, and an interior attractor in the model (3). Moreover, the existence of a heteroclinic curve that acts as a separatrix curve between the basin of attractions of multiple attractors is proved for both models. However, when this curve is broken by changing parameter values, the total extinction of both populations occurs in the model (1), while in the model (2) extinction of the prey population can be avoided for certain initial conditions above the Allee effect threshold.

Acknowledgement

The authors are grateful to the anonymous referee who made several useful suggestions that improved the quality of this paper.

References

[1] S. M. A. Al-Momen, R.K. Naji, *The Dynamics of Modified Leslie-Gower Predator-Prey Model Under the Influence of Nonlinear Harvesting and Fear Effect*, Iraqi J. Sci. **63(1)** (2022), 259–282.

[2] L. Berec, E. Angulo, F. Courchamp, *Multiple Allee effects and population management*, Trends Ecol. Evol. **22** (2007), 185–191.

[3] W.C. Allee, *Animal Aggregations: A Study in General Sociology*, University of Chicago Press, Chicago, 1931.

[4] B. Belew, D. Melese, *Modeling and Analysis of Predator-Prey Model with Fear Effect in Prey and Hunting Cooperation among Predators and Harvesting*, Journal of Applied Mathematics, vol. 2022, Article ID 2776698, 14 pages, 2022.

[5] R. Bogdanov, *Bifurcations of a limit cycle for a family of vector fields on the plane*, Sel. Math. Sov. **1** (1981), 373–388.

[6] R. Bogdanov, *Versal deformations of a singular point on the plane in the case of zero eigen-values*, Sel. Math. Sov. **1** (1981), 389–421.

[7] J. Chen, J. Huang, S. Ruan, J. Wang, *Bifurcations of invariant tori in predator–prey models with seasonal prey harvesting*, SIAM J. Appl. Math. **73 (5)** (2013), 1876–1905.

[8] C. Chicone, *Ordinary Differential Equations with Applications*, in: Texts in Applied Mathematics., **34**, World Scientific, Springer-Verlag New York, 2006.

[9] C. W. Clark, *Mathematical Bioeconomics: The Optimal Management of Renewable Resources*, Wiley, New York, 1976.

[10] B.D. Dalziel, E. Thomann, J. Medlock, P. De Leenheer, *Global analysis of a predator–prey model with variable predator search rate*, J. Math. Biol. **81** (2020), 159–183.

[11] T. Das, R.N. Mukherjee, K.S. Chaudhuri, *Bioeconomic harvesting of a prey–predator fishery*, J. Biol. Dyn. **3 (5)** (2009), 447–462.

[12] J.H.P. Dawes, M.O. Souza, *A derivation of Holling's type I, II and III functional responses in predator–prey systems*, J. Theor. Biol. **327** (2013), 11–22.

[13] A. Dhooge, W. Govaerts, Yu.A. Kuznetsov, H.G.E. Meijer, B. Sautois, *New features of the software MatCont for bifurcation analysis of dynamical systems*, MCMDS **14 (2)** (2008), 147–175.

[14] N.K. Dulvy, *Extinction vulnerability in marine populations*, Fish Fish. **4** (2003), 25–64.

[15] K. M. Dunmall, J. D. Reist, E. C. Carmack, J. A. Babaluk, M. P. Heide-Jørgensen, M. F. Docker, *Pacific salmon in the Arctic: Harbingers of change*, in Responses of Arctic Marine Ecosystems to Climate Change, F. J. Mueter, D. M. S. Dickson, H. P. Huntington, J. R. Irvine, E. A. Logerwell, S. A. MacLean, L. T. Quakenbush, C. Rosa, Eds. (Alaska Sea Grant Univ. of Alaska, Fairbanks, (2013), 141–163.

[16] T. Erhardt, R. Weder, *Shark hunting: On the vulnerability of resources with heterogeneous species*, Resour. Energy Econ. **61** (2020), 101181.

[17] H.I. Freedman, *Deterministic Mathematical Models in Population Ecology*, Marcel Dekker, New York, 1980.

[18] H.I. Freedman, G.S.K. Wolkowicz, *Predator-prey systems with group defense: the paradox of enrichment revisited*, Bull. Math. Biol. **48** (1986), 493–508.

[19] T.C. Gard, *Uniform persistence in multispecies population models*, Math. Biosci. **85** (1987), 93–104.

[20] S. Georgette, M. Coffing, C. Scott, and C. Utermohle, *The subsistence harvest of seals and sea lions by Alaska Natives in the Norton Sound-Bering Strait region, Alaska, 1996-97* Alaska Department of Fish and Game, Division of Subsistence, Technical Paper No. 242. 88 p.

[21] E. Gonzalez-Olivares, H. Meneses-Alcay, B. González-Yañez, J. Mena-Lorca, A. Rojas-Palma, R. Ramos Jiliberto, *Multiple stability and uniqueness of the limit cycle in a Gause-type predator–prey model considering the Allee effect on prey*, Nonlinear Anal. Real World Appl. **12** (2011), 2931–2942.

[22] R.P. Gupta, P. Chandra, *Bifurcation analysis of modified Leslie–Gower predator–prey model with Michaelis–Menten type prey harvesting*, J. Math. Anal. Appl. **398 (1)** (2013), 278–295.

[23] C.S. Holling, *The components of predation as revealed by a study of small-mammal predation of the European sawfly*, Can. Entomol. **91** (1959), 293–320.

[24] C.S. Holling, *Some characteristics of simple types of predation and parasitism*, Can. Entomol. **91** (1959), 385–398.

[25] Hu, D., Cao, H., *Stability and bifurcation analysis in a predator-prey system with Michaelis-Menten type predator harvesting* Nonlinear Anal. R. World Appl. **33** (2017), 58–82.

[26] V. Hutson, *A theorem on average Liapunov functions*, Monatsh. Math. **98** (1984) 267–275.

[27] A. R. Jamil, R. K. Naji, *Modeling and Analysis of the Influence of Fear on the Harvested Modified Leslie-Gower Model Involving Nonlinear Prey Refuge*, Mathematics **10** (2022), 2857.

[28] S.V. Krishna, P.D.N. Srinivasu, B. Kaymackcalan, *Conservation of an ecosystem through optimal taxation*, Bull. Math. Biol. **60** (1998), 569–584.

[29] U. Kumar, P. S. Mandal, *Role of Allee effect on prey–predator model with component Allee effect for predator reproduction*, Math. Comput. Simul. **193** (2022), 623–665.

[30] A. Y. Kuznetsov, *Elements of Applied Bifurcation Theory*, Appl. Math. Sci., 112. Springer-Verlag, New York, 2004.

[31] L. Lai, X. Yu, M. He, Z. Li, *Impact of Michaelis–Menten type harvesting in a Lotka–Volterra predator–prey system incorporating fear effect*, Advances in Difference Equations **320** (2020), 1–22.

[32] M. Liermann, R. Hilborn, *Depensation: evidence, models and implications*, Fish and Fisheries **2** (2001), 33–58

[33] A.J. Lotka, *Elements of Physical Biology*, Williams & Wilkins, Baltimore, 1925.

[34] H. Molla, Md. Rahman, S. Sabiar Sarwardi, *Dynamics of a predator-prey model with Holling Type II functional response incorporating a prey refuge depending on both the species*, Int. J. Nonlinear Sci. Numer. Simul. **20** (2019), 89–104.

[35] B. Mondal, S. Roy, U. Ghosh, P.K. Tiwari, *A systematic study of autonomous and nonautonomous predator-prey models for the combined effects of fear, refuge, cooperation and harvesting*, Eur Physi J Plus 137:724 (2023).

[36] R.A. Myers, N.J. Barrowman, J.A. Hutchings, A.A. Rosenberg, *Population dynamics of exploited fish stocks at low population levels*, Science **269** (1995), 1106–1108.

[37] R. D. M. Nash, M. Dickey-Collas, L. T. Kell, *Stock and recruitment in North Sea herring (Clupea harengus); compensation and depensation in the population dynamics*, Fisheries Research **95** (2009), 88–97.

[38] E.M. Olsen, M.R. Heupel, C.A. Simpfendorfer, E. Moland, *Harvest selection on Atlantic cod behavioural traits: implications for spatial management*, Ecology and Evolution **2** (2012), 1549–1562

[39] L. Perko, *Differential Equations and Dynamical Systems*, third edition, Springer, New York, 2001.

[40] K. Raab, *The European anchovy (Engraulis encrasicolus) increase in the North Sea* (2013) PhD thesis, Wageningen University, Wageningen.

[41] Z. Shang, Y. Qiao, L. Duan, J. Miao, *Bifurcation analysis in a predator–prey system with an increasing functional response and constant-yield prey harvesting*, Mathematics and Computers in Simulation **190** (2021), 976–1002.

[42] P. Stephens, W. Sutherland, R. Freckleton, *What is the Allee effect?*, Oikos **87** (1999), 185–190.

[43] J. Su, *Degenerate Hopf bifurcation in a Leslie–Gower predator–prey model with predator harvest*, Advances in Difference Equations **194** (2020), 1–19.

[44] F. Takens, *Forced oscillations and bifurcation*, in: Applications of Global Analysis I, in: Comm. Math. Inst. Rijksuniversitat Utrecht. **3** (1974), 1–59.

[45] V. Volterra, *Fluctuations in the abundance of a species considered mathematically*, Nature **118 (2972)** (1926), 558–560.

[46] S. Wiggins, *Introduction to Applied Nonlinear Dynamical Systems and Chaos*, Springer, New York, 1990.

[47] G.S.K. Wolkowicz, *Bifurcation Analysis of a Predator-Prey System Involving Group Defence*, SIAM J. on Appl. Math. **48 (3)** (1988), 592–606.

[48] D. Xiao, L.S. Jennings, *Bifurcations of a ratio-dependent predator–prey system with constant rate harvesting*, SIAM J. Appl. Math. **65 (3)** (2005), 737–753.

[49] E. S. Zbarsky, *Phase Plane and Slope Field apps* (https://github.com/MathWorks-Teaching-Resources/Phase-Plane-and-Slope-Field/releases/tag/v1.1.1), GitHub.

[50] Z. Zhang, T. Ding, W. Huang, Z. Dong, *Qualitative Theory of Differential Equations*, Transl. Math. Monogr., vol. **101**, Amer. Math. Soc., Providence, RI, 1992.